

EFFECT OF TIP-SPEED RATIO ON INDUCED
VELOCITIES NEAR A LIFTING ROTOR

by

Harry H. Heyson

Thesis submitted to the Graduate Faculty of the
Virginia Polytechnic Institute
in candidacy for the degree of
MASTER OF SCIENCE
in
Aeronautical Engineering

APPROVED:

APPROVED:

Director of Graduate Studies

Head of Department

Dean of Engineering

Supervisor or Major Professor

February 1, 1958

Blacksburg, Virginia

CONTENTS

I. Symbols	5
II. Introduction	7
III. Theory	11
Assumed wake	11
Induced velocities of outer wake	13
Induced velocities of inner wake	16
Numerical calculations	24
Vorticity distribution of the rotor	26
IV. Discussion of calculated results	31
V. Comparison with experiment	35
VI. Conclusions	38
VII. Summary	39
VIII. Acknowledgements	40
IX. Bibliography	41
X. Vita	44
XI. Appendix	45
Tables	50
Figures	65

TABLE I

I. Limiting values of are tangent in equation (22)	50
II. Calculated values of induced-velocity ratio, w/w_0 , in the lateral plane of a rotor with unit sine ψ vorticity, $X = \tan^{-1} k = 63.43^\circ$	51
III. Calculated values of induced-velocity ratio, w/w_0 , in the lateral plane of a rotor with unit sine ψ vorticity, $X = \tan^{-1} k = 70.97^\circ$	52
IV. Calculated values of induced-velocity ratio, w/w_0 , in the lateral plane of a rotor with unit sine ψ vorticity, $X = \tan^{-1} k = 84.23^\circ$	53

FIGURE

1. Rotor wake system	53
2. Contours of induced-velocity ratio, w/w_0 , shown as the individual contributions of the inner and outer wakes in lateral plane of a rotor having a radially uniform unit sin ψ vorticity distribution. $X = \tan^{-1} k = 70.97^\circ$	65
3. Contours of induced-velocity ratio, w/w_0 , in the lateral plane in the immediate vicinity of a rotor having a radially uniform unit sin ψ vorticity distribution.	66
4. Contours of induced-velocity ratio, w/w_0 , outside the wake in the lateral plane of a rotor with a radially uniform unit sin ψ vorticity distribution.	69

5. Contours of induced-velocity ratio, w/w_0 , in the lateral plane of a rotor having a triangular, circularly symmetrical vorticity distribution.	72
6. Comparison, with reference 5, of induced velocities due to asymmetry, lateral axis.	75
7. Comparison, in the lateral plane, of theory and the measurements of reference 11.	77
8. Comparison, along the lateral axis, of theory and the measurements of reference 11.	80
9. Comparison of calculated time-averaged induced velocities with effective induced velocities as determined by pressure distribution measurements on a rotor blade (ref. 15). $\mu = 0.50$	81

I. SYMBOLS

- \bar{a} vector distance from P to vortex element (see fig. 1), feet.
- A $\frac{1}{R}(x \cos \psi + y \sin \psi)$.
- B $\frac{1}{R}(z \cos \chi - x \sin \chi)$.
- C $\frac{1}{R}(y \cos \psi - x \sin \psi) \cos \chi - z \sin \chi \sin \psi$.
- $f(\psi)$ Fourier sine-cosine series (normalized with respect to the constant term) describing the azimuthwise variation of vorticity in the outer wake. The negative derivative of $f(\psi)$ describes the corresponding vorticity in the inner wake.
- $\bar{i}, \bar{j}, \bar{k}$ unit vectors along x , y , and z axes, respectively.
- L distance along wake, measured from tip-path plane, (see fig. 1), feet.
- P arbitrary point in space.
- \bar{v} vector induced velocity at P , feet per sec.
- r radius of vortex element, measured parallel to tip-path plane from wake axis (see fig. 1), feet.
- R rotor radius, feet.
- R_c distance between P and edge of rotor disk at ψ (see fig. 1), feet, $\sqrt{R^2 + x^2 + y^2 + z^2} - R\alpha$.
- R_0 distance from P to center of rotor, feet, $\sqrt{x^2 + y^2 + z^2}$.
- \bar{s} vector length of vortex element, feet.
- x, y, z coordinates of P (see fig. 1), feet.
- u, v, w induced-velocity components along x , y , and z axes, respectively, feet per sec.

- U velocity of blade element, feet per sec.
- V forward speed of rotor, feet per sec.
- w_0 normal component of induced velocity at center of symmetric, uniformly loaded rotor, positive upward, feet per sec.
- α angle of attack of rotor tip-path plane, radians.
- Γ circulation, square feet per sec.
- λ rotor inflow ratio, $\frac{V \sin \alpha + w_0}{\Omega R}$.
- μ rotor tip-speed-ratio, $\frac{V \cos \alpha}{\Omega R}$.
- ρ mass density of air, slugs per cubic foot.
- χ wake skew angle, measured positively from the negative z-axis to the axis of rotor wake (see fig. 1), degrees.
- ψ azimuth angle, measured in direction of rotation from downwind position, radians or degrees.
- Ω rotor rotational speed, radians per sec.

Primes indicate nondimensionalization with respect to R .

II. INTRODUCTION

The widespread use of the helicopter today is a result primarily of its hovering and vertical flight capabilities. The penalty for vertical flight capability is high, since the relatively low speed of the retreating blade requires high angles of attack resulting in blade stall which severely limits the maximum forward speed of the helicopter. Attempts to achieve a more reasonable combination of hovering and forward-flight characteristics have led to a staggering number and variety of designs, ranging from "unloaded-rotor" convertiplanes to VTOL fighters. Excluding jet-powered VTOL designs, these hybrid aircraft usually have at least one important feature in common - that is, the presence of a wing operating in the wake of lifting rotors. The performance and stability of the entire aircraft is therefore intimately related to the mutual interference between the wing and the rotors.

The flow-field in the vicinity of a conventional wing has been studied extensively for years and a great deal of information is readily available. Unfortunately, the counterpart does not exist for a lifting rotor. This is partially the result of the mathematical complexity of rotor-wake calculations. However, the main reason is that even the simplest estimate of the induced flow distribution yields adequate results when computing only the overall performance of an isolated rotor. (See, for example, references 1 and 2, where a uniform induced-velocity distribution is shown to yield almost the same results as a linearly varying induced velocity.)

The advent of the practical helicopter focused considerable attention on the high rotor-blade vibration levels encountered during certain flight conditions. An attempt to explain these vibrations led Coleman, Feingold, and Stempin (ref. 3) to investigate the distribution of induced velocity in the plane of the rotor. This pioneer analysis was based upon a concept of the rotor wake originally proposed years before by Glauert (ref. 4), and which still forms the basis of almost all rotor induced-flow theory. The investigation of reference 3 succeeded in establishing the general nature of the variation of induced velocity along the longitudinal center line of a uniformly loaded rotor.

A few years later Drees (ref. 5) examined the flow at several points in the rotor disk. The most notable result of this investigation was an estimate of the lateral asymmetry of the induced velocities which was obtained by a means of a crude approximation to the wake. This is the only available paper which has considered lateral asymmetry of the vortex wake. The method, however, can not be extended to an arbitrary point in space.

At about the same time, Mangler and Squire (ref. 6) published the results of their own investigation which was unique in that it considered the rotor flow problem from the viewpoint of circular wing theory. This investigation showed clearly the large effect on the flow which results from nonuniformity of loading. Unfortunately, this result was generally overlooked due to the lack of reliable experimental verification.

More recently, Castles and DeLeeuw (ref. 7) succeeded in obtaining the induced velocities throughout the longitudinal plane of symmetry of

a rotor with uniform disk loading by numerically integrating the effects of the series of vortex rings comprising the wake. This investigation provided, for the first time, induced velocities at locations of interest for interference problems and formed a basis for many succeeding investigations. (See, also, refs. 8 and 9 where Castles and others have extended this work to other locations by means of automatic digital computers and a magnetic analog.)

The usefulness of the preceding papers was severely limited by an almost total lack of reliable experimental information. This was due in large part to the very practical difficulties of measuring the flow angles and velocities either in flight or in small-scale wind-tunnels. The need for such information led to an extensive flow-survey program in the NACA's Langley full-scale tunnel. Reference 10 presents a few preliminary results from this investigation, and the bulk of the work was presented later in reference 11. The salient point of this investigation was that, in the forward regions of the flow which are not materially affected by the roll-up of the rotor wake, the theoretically calculated flows were in reasonable agreement with the measured flow, provided that the disk-load distribution assumed was reasonably close to that which actually exists on the rotor. In addition, a method of superposition was given, by which it is possible to adjust the available uniformly loaded rotor calculations to correspond to any arbitrary axisymmetric load distribution.

One feature observed during the course of the investigation of references 10 and 11 was a pronounced asymmetry of flow as a function of

tip-speed ratio. Such an asymmetry would be expected because the advancing and retreating blades of the rotor operate at very different velocities and angles of attack. However, existing theory is not capable of computing this effect since the wake is generally assumed to be symmetrical. This shortcoming of theory could be serious since the side-to-side differences in flow may result in changes in the rotor-wing interference causing large rolling moments on single rotor convertiplanes or even large performance changes on certain twin-rotor machines.

The present investigation studies the effect of tip-speed-ratio and the associated wake asymmetry on the induced velocities near a lifting rotor. The analysis is based on an assumed wake which is a logical extension of that used in previous investigations. Equations are developed for all three induced-velocity components in terms of an arbitrary azimuthwise variation of blade circulation. An automatic digital computer was used to integrate the equation for the normal component of induced velocity in the lateral plane of a rotor having a sinusoidal variation of circulation. The numerical results are presented in both tabular and chart form. Comparisons are made both with the limited results of Drees (ref. 5) and with the measurements of reference 11.

III. THEORY

Assumed wake. - Rotary wing induced flows are generally calculated in the same manner as the flows of wings, that is, by integrating the effect of all the vortices shed behind the lifting surface. The present analysis assumes the wake to be essentially the same as that of references 3-5 and 7-11.

The major characteristics of the assumed wake and the assumptions made are as follows:

1. The blade circulation is uniform along the radius but varies with azimuth angle in some predetermined fashion.
2. The tip vortices are carried downward at a uniform rate of ΩR , and rearward at a uniform rate of $\mu \Omega R$, and thus lie as helices upon the surface of an elliptic cylinder which is skewed back from the tip-path-plane axis at an angle $X = \tan^{-1} \frac{\mu}{\lambda}$. (See fig. 1(a).)
3. The vortex spacing along the wake is sufficiently close that the vorticity may be considered uniformly distributed along the surface of the skewed cylinder.
4. The effects of the axial component of vorticity in the wake and of the bound vortices on the blades are negligibly small.

The effect of these assumptions should not greatly limit the usefulness of the results. The first assumption is not a severe handicap since reference 11 shows that these results may be converted by superposition to correspond with other loadings. The second assumption requires that the vortices be carried off at the mean flow rate rather

than with the local flow, and thus incurs considerable error at very low speeds where only the induced velocities are present (see ref. 11). At higher speeds, this means that the roll-up of the wake is neglected. However, this affects only the rearward portion of the flow (ref. 11). The third assumption restricts the analysis to time-averaged mean velocities rather than the instantaneous induced velocities responsible for the loading variations shown in references 12 and 13. This facet of the problem will be examined at greater length in a subsequent portion of this thesis. Finally, such experimental results as are available give no evidence that the axial vorticity is important, and the major portion of the bound-vortex effects have been shown in references 5 and 10 to be small when time-averaged.

In the present case, the essential modification to the wake of previous analyses is that the strength of the vorticity is allowed to vary with azimuth position. This cylindrical wake with varying vorticity will be referred to in the remainder of this thesis as the "outer wake." (See fig. 1(a).)

Now if the vorticity in the outer wake varies with azimuth angle, the theorem that vorticity cannot end in space requires the presence of additional radial vorticity inside the outer wake. Thus an "inner wake," a solid skewed cylinder of radial vorticity (fig. 1(b)), is formed. The strength of this vorticity is equal to the negative of the rate of change of the vorticity of the outer wake.

In the succeeding sections, the induced-velocity contributions of the inner and outer wakes are developed separately as a matter of

convenience. The total induced velocity is, of course, the sum of both contributions.

Induced velocities of outer wake. - The induced velocities may be found by integrating the Biot-Savart law over the wake. The Biot-Savart law is

$$d\bar{v} = \frac{1}{4\pi} \frac{d\Gamma}{dL} \frac{d\bar{s} \times \bar{a}}{|\bar{a}|^3} dL, \quad (1)$$

where the following may be determined from figure 1(a) by inspection:

$$\bar{s} = \bar{i}(R \cos \psi + L \sin \chi) + \bar{j}(R \sin \psi) + \bar{k}(-L \cos \chi)$$

$$d\bar{s} = [\bar{i}(-R \sin \psi) + \bar{j}(R \cos \psi) + \bar{k}0] d\psi$$

$$\bar{a} = \bar{i}(R \cos \psi + L \sin \chi - x) + \bar{j}(R \sin \psi - y) + \bar{k}(-L \cos \chi - z).$$

Substitution of these values in equation (1) and integrating yields

$$\bar{i} = \frac{R}{4\pi} \int_0^{2\pi} \int_0^\infty \frac{d\Gamma}{dL} \begin{vmatrix} \bar{i} & \bar{j} & \bar{k} \\ -\sin \psi & \cos \psi & 0 \\ R \cos \psi + L \sin \chi - x & R \sin \psi - y & -L \cos \chi - z \end{vmatrix} \frac{dL d\psi}{[(R \cos \psi + L \sin \chi - x)^2 + (R \sin \psi - y)^2 + (-L \cos \chi - z)^2]^{\frac{3}{2}}}, \quad (2)$$

from which the normal, or \bar{k} , component of induced velocity is

$$w = \frac{R}{4\pi} \int_0^{2\pi} \int_0^\infty \frac{dr}{dL} \frac{x \cos \psi + y \sin \psi - R - L \sin \chi \cos \psi}{\left[R^2 + x^2 + y^2 + z^2 - 2R(x \cos \psi + y \sin \psi) + 2L(z \cos \chi - x \sin \chi + R \sin \chi \cos \psi) + L^2 \right]^{\frac{3}{2}}} dL d\psi. \quad (3)$$

The integration with respect to L may be accomplished with the aid of items 162 and 170 of reference 14, or

$$w = \frac{R}{4\pi} \int_0^{2\pi} \frac{d\Gamma}{dL} \frac{(x \cos \psi + y \sin \psi)(z \cos \chi - x \sin \chi + R \sin \chi \cos \psi) + \sin \chi \cos \psi \left[\frac{L z \cos \chi - x \sin \chi + R \sin \chi \cos \psi}{L + R^2 + x^2 + y^2 + z^2 - 2R(x \cos \psi + y \sin \psi)} \right]}{\left(R^2 + x^2 + y^2 + z^2 - 2R(x \cos \psi + y \sin \psi) - (z \cos \chi - x \sin \chi + R \sin \chi \cos \psi) \right)^2} d\Gamma \Big|_0^\infty. \quad (4)$$

After substituting limits and combining terms, equation (4) reduces to

$$w = \frac{R}{4\pi} \int_0^{2\pi} \frac{(x \cos \psi + y \sin \psi - R) - \sin \chi \cos \psi \left[\frac{R^2 + x^2 + y^2 + z^2 - 2R(x \cos \psi + y \sin \psi)}{R^2 + x^2 + y^2 + z^2 - 2R(x \cos \psi + y \sin \psi)} \right]}{\left[R^2 + x^2 + y^2 + z^2 - 2R(x \cos \psi + y \sin \psi) + z \cos \chi - x \sin \chi + R \sin \chi \cos \psi - R^2 + x^2 + y^2 + z^2 - 2R(x \cos \psi + y \sin \psi) \right]} d\psi. \quad (5)$$

Introducing nondimensional coordinates and noting that $\sqrt{R^2 + x^2 + y^2 + z^2 + 2R(x \cos \psi + y \sin \psi)} = R_C$ results in

$$w = -\frac{1}{4\pi} \int_0^{2\pi} \frac{d\Gamma}{dL} \frac{1 - (x' \cos \psi + y' \sin \psi) + R_C' \sin \chi \cos \psi}{\left[R_C' + (\cos \psi - x') \sin \chi + z' \cos \chi R_C' \right]} d\psi. \quad (6)$$

At the center of the rotor, $x' = y' = z' = 0$, so that equation (6) reduces to

$$w = -\frac{1}{4\pi} \int_0^{2\pi} \frac{d\Gamma}{dL} d\psi. \quad (7)$$

Specifying now that $\frac{d\Gamma}{dL}$ may be expressed as $\left(\frac{d\Gamma}{dL}\right)_0 f(\psi)$, where $\left(\frac{d\Gamma}{dL}\right)_0$ is the constant part of the vorticity and $f(\psi)$ is a Fourier series in ψ , normalized with respect to the constant term, it is evident that the only term which can produce a normal induced velocity at the center of the rotor is the constant term. The induced velocity at the center will be

$$w_0 = -\frac{1}{2} \left(\frac{d\Gamma}{dL}\right)_0, \quad (8)$$

so that, finally,

$$\frac{w}{w_0} = \frac{1}{2\pi} \int_0^{2\pi} f(\psi) \frac{[1 - (x' \cos \psi + y' \sin \psi) + R_c' \sin \chi \cos \psi]}{[R_c' + (\cos \psi - x') \sin \chi + z' \cos \chi] R_c'} d\psi. \quad (9)$$

The longitudinal, or i , component of the induced velocity is, from equation (2)

$$u = \frac{-R}{4\pi} \int_0^{2\pi} \frac{d\Gamma}{dL} \frac{(z + L \cos \chi) \cos \psi dL d\psi}{[R^2 + x^2 + y^2 + z^2 - 2R(x \cos \psi + y \sin \psi) + 2L(z \cos \chi - x \sin \chi + R \sin \chi \cos \psi) + L^2]^{\frac{3}{2}}}. \quad (10)$$

The integration follows in exactly the same manner as for the normal component. The final expression is found to be

$$\frac{u}{w_0} = -\frac{1}{2\pi} \int_0^{2\pi} f(\psi) \frac{(z' + R_c' \cos \chi) \cos \psi d\psi}{[R_c' + z' \cos \chi + (\cos \psi - x') \sin \chi]^{R_c'}}. \quad (11)$$

From equation (2), the lateral, or \bar{j} , component is

$$v = \frac{-R}{4\pi} \int_0^{2\pi} \left| \int_0^\infty \frac{d\Gamma}{dL} \right| \frac{(z + L \cos \chi) \sin \psi dL d\psi}{[R^2 + x^2 + y^2 + z^2 - 2R(x \cos \psi + y \sin \psi) + 2L(z \cos \chi - x \sin \chi + R \sin \chi \cos \psi) + L^2]^{\frac{3}{2}}}. \quad (12)$$

It is apparent that equation (12) differs from equation (10) only by a factor $\tan \psi$ which does not enter into the integration with respect to L . Thus, the final expression for the lateral component of induced velocity may be written immediately, on comparison with equation (11), as

$$\frac{v}{w_0} = -\frac{1}{2\pi} \int_0^{2\pi} f(\psi) \frac{(z' + R_c' \cos \chi) \sin \psi d\psi}{[R_c' + z' \cos \chi + (\cos \psi - x') \sin \chi]^{R_c'}}. \quad (13)$$

Induced velocities of inner wake.- The induced velocities of the inner wake are found, as before, by integrating the Biot-Savart law, where now, from figure 1(b),

$$\bar{s} = \bar{i}(r \cos \psi + L \sin \chi) + \bar{j}(r \sin \psi) + \bar{k}(-L \cos \chi)$$

$$ds = \bar{i}(\cos \psi) + \bar{j}(\sin \psi) + \bar{k}(0) dr$$

$$\bar{a} = \bar{i}(r \cos \psi + L \sin \chi - x) + \bar{j}(r \sin \psi - y) + \bar{k}(-L \cos \chi - z).$$

Substituting these expressions into equation (1) and integrating yields

$$\bar{q} = \frac{-1}{4\pi} \int_0^{2\pi} \int_0^R \left[\frac{\partial}{\partial \psi} \left(\frac{d\Gamma}{dL} \right) (r \cos \psi + L \sin \chi - x) (r \sin \psi - y) (-L \cos \chi - z) \right] dL dr d\psi$$

$$+ \frac{1}{2} \left[(r \cos \psi + L \sin \chi - x)^2 + (r \sin \psi - y)^2 + (-L \cos \chi - z)^2 \right], \quad (14)$$

from which the normal, or \bar{k} , component of induced velocity is

$$w = \frac{1}{4\pi} \int_0^{2\pi} \int_0^R \left[\frac{d(d\Gamma)/dL}{d\psi} [x \sin \psi - y \cos \psi - L \sin \chi \sin \psi] dL dr d\psi \right]$$

$$+ \frac{1}{2} \left[r^2 + x^2 + y^2 + z^2 - 2r(x \cos \psi + y \sin \psi) + 2L(z \cos \chi - x \sin \chi + r \sin \chi \cos \psi) + L^2 \right]^{\frac{3}{2}}, \quad (15)$$

The integration of equation (14) with respect to L may be accomplished with the aid of items 162 and 170 of reference 14, thus

$$w = \frac{1}{4\pi} \int_0^{2\pi} \int_0^R \frac{d}{d\psi} \left(\frac{d\Gamma}{dL} \right) \frac{(x \sin\psi - y \cos\psi)(z \cos\chi - x \sin\chi + r \sin\chi \cos\psi) + [z \cos\chi - x \sin\chi + r \sin\chi \cos\psi] L + x^2 + y^2 + z^2 - 2r(x \cos\psi + y \sin\psi) \sin\chi \sin\psi}{[r^2 + x^2 + y^2 + z^2 - 2r(x \cos\psi + y \sin\psi)]^2 \sqrt{r^2 + x^2 + y^2 + z^2 - 2r(x \cos\psi + y \sin\psi) + 2L(z \cos\chi - x \sin\chi + r \sin\chi \cos\psi) + L^2}} dr d\psi. \quad (16)$$

Upon substituting limits, equation 16 reduces to

$$w = \frac{1}{4\pi} \int_0^{2\pi} \int_0^R \frac{\frac{d}{d\psi} \left(\frac{d\Gamma}{dL} \right)}{\sqrt{r^2 + x^2 + y^2 + z^2 - 2r(x \cos\psi + y \sin\psi) + z \cos\chi - x \sin\chi + r \sin\chi \cos\psi}} \frac{x \sin\psi - y \cos\psi - \sin\chi \sin\psi \sqrt{r^2 + x^2 + y^2 + z^2 - 2r(x \cos\psi + y \sin\psi)}}{\sqrt{r^2 + x^2 + y^2 + z^2 - 2r(x \cos\psi + y \sin\psi) + z \cos\chi - x \sin\chi + r \sin\chi \cos\psi}} dr d\psi. \quad (17)$$

The integration of equation (17) with respect to r is somewhat involved, and is carried out in general terms in the appendix. Substituting into equations (A3) and (A12), and noting the identity

$$-2(\sin\chi \cos\psi - 1)(x \cos\psi + y \sin\psi)(z \cos\chi - x \sin\chi) - (x^2 + y^2 + z^2)(\sin^2\chi \cos^2\psi - 1)$$

$$- (x \cos\psi + y \sin\psi) - (z \cos\chi - x \sin\chi)^2 = [(y \cos\psi - x \sin\psi)\cos\chi - z \sin\chi \sin\psi]^2, \quad (18)$$

yields

$$w = \frac{1}{4\pi} \int_0^{2\pi} \frac{\frac{d}{d\psi} \left(\frac{dR}{dL} \right)}{1 - \sin^2 x \cos^2 \psi} \tan^{-1} \frac{(1 - \sin x \cos y) \sqrt{r^2 + x^2 + y^2 + z^2 - 2r(x \cos \psi + y \sin \psi) - R}}{(y \cos \psi - x \sin \psi) \cos x - z \sin x \sin y}$$

$$+ \frac{\sin^2 x \sin y \cos \psi}{1 - \sin^2 x \cos^2 \psi} \ln \frac{1}{r^2 + x^2 + y^2 + z^2 - 2r(x \cos \psi + y \sin \psi) + (z \cos x - x \sin y) + r \sin x \cos y} \left| \begin{array}{l} \\ \\ \end{array} \right. \\ + \frac{\sin x \sin y}{1 - \sin^2 x \cos^2 \psi} \ln 2 \left| r - (x \cos \psi + y \sin \psi) - \frac{r^2 + x^2 + y^2 + z^2 - 2r(x \cos \psi + y \sin \psi) - R}{(y \cos \psi - x \sin \psi) \cos x - z \sin x \sin y} \right| \left| \begin{array}{l} \\ \\ \end{array} \right. \quad (19)$$

Upon substituting limits, this becomes

$$w = \frac{1}{4\pi} \int_0^{2\pi} \frac{\frac{d}{d\psi} \left(\frac{dR}{dL} \right)}{1 - \sin^2 x \cos^2 \psi} \tan^{-1} \frac{(1 - \sin x \cos y) \sqrt{R^2 + x^2 + y^2 + z^2 - 2R(x \cos \psi + y \sin \psi) - R}}{(y \cos \psi - x \sin \psi) \cos x - z \sin x \sin y} \\ - \frac{2 \cos x}{1 - \sin^2 x \cos^2 \psi} \tan^{-1} \frac{(1 - \sin x \cos y) \sqrt{x^2 + y^2 + z^2 + (x \cos \psi + y \sin \psi) + (z \cos x - x \sin y)}}{(y \cos \psi - x \sin \psi) \cos x - z \sin x \sin y} \\ + \frac{\sin^2 x \sin y \cos \psi}{1 - \sin^2 x \cos^2 \psi} \ln \frac{(x \cos \psi + y \sin \psi) + (z \cos x - x \sin y) + R \sin x \cos y}{x^2 + y^2 + z^2 + (z \cos x - x \sin x)} \\ + \frac{\sin x \sin y}{1 - \sin^2 x \cos^2 \psi} \ln \frac{(x \cos \psi + y \sin \psi) + (R^2 + x^2 + y^2 + z^2 - 2R(x \cos \psi + y \sin \psi) - R)}{x^2 + y^2 + z^2 + (x \cos \psi + y \sin \psi)} \quad (20)$$

which becomes, upon nondimensionalizing,

$$\frac{w}{w_0} = \frac{-1}{2\pi} \int_0^{2\pi} \frac{df(\psi)}{d\psi} \left\{ \left[\frac{2 \cos x}{1 - \sin^2 x \cos^2 \psi} \tan^{-1} \left[\frac{(1 - \sin x \cos \psi)(R_c' - 1) + A + B}{C} \right] \right] \right. \\ \left. + \frac{\sin^2 x \sin \psi \cos \psi}{1 - \sin^2 x \cos^2 \psi} \ln \left| \frac{R_c' + B + \sin x \cos \psi}{R_0' + B} \right| + \frac{\sin x \sin \psi}{1 - \sin^2 x \cos^2 \psi} \ln \left| \frac{R_c' + A - 1}{R_0' + A} \right| \right\} d\psi. \quad (21)$$

In general, it will be found convenient to combine the two inverse tangent terms of equation (21) by means of item 648 of reference 14, yielding

$$\frac{w}{w_0} = \frac{-1}{2\pi} \int_0^{2\pi} \frac{df(\psi)}{d\psi} \left\{ \frac{2 \cos x}{1 - \sin^2 x \cos^2 \psi} \tan^{-1} \left[\frac{R_0'(R_c' - 1)(1 - \sin x \cos \psi)}{R_0'(R_c' - 1)^2 + (A + B)(R_c' + R_0' - 1)(1 - \sin x \cos \psi) + (A + B)^2 + C^2} \right] \right. \\ \left. + \frac{\sin^2 x \sin \psi \cos \psi}{1 - \sin^2 x \cos^2 \psi} \ln \left| \frac{R_c' + B + \sin x \cos \psi}{R_0' + B} \right| + \frac{\sin x \sin \psi}{1 - \sin^2 x \cos^2 \psi} \ln \left| \frac{R_c' + A - 1}{R_0' + A} \right| \right\} d\psi. \quad (22)$$

In certain cases, the argument of the inverse tangent term becomes indeterminate. The limiting value, however, may be found by the repeated application of L'Hospital's rule. Limiting values for a few of the more important cases are given in table I.

The longitudinal, or \bar{i} , component of induced velocity is, from equation (14),

$$u = \frac{-1}{4\pi} \int_0^{2\pi} \int_0^R \int_0^\infty \frac{\frac{d}{d\psi} \left(\frac{d\Gamma}{dL} \right) (z + L \cos X) \sin \psi \ dL \ dr \ d\psi}{[r^2 + x^2 + y^2 + z^2 - 2r(x \cos \psi + y \sin \psi) + 2L(z \cos X - x \sin X + r \sin X \cos \psi) + L^2]^2}. \quad (23)$$

Equation (23) may be integrated with respect to L to yield

$$u = \frac{-1}{4\pi} \int_0^{2\pi} \int_0^R \frac{\frac{d}{d\psi} \left(\frac{d\Gamma}{dL} \right) [\sin \psi] \left[z + \cos X \sqrt{r^2 + x^2 + y^2 + z^2 - 2r(x \cos \psi + y \sin \psi)} \right] dr \ d\psi}{\sqrt{r^2 + x^2 + y^2 + z^2 - 2r(x \cos \psi + y \sin \psi) + z \cos X - x \sin X + r \cos \psi \sin X}}. \quad (24)$$

Integrating with respect to r , by means of equations (A3) and (A12) of the appendix, results in

$$\begin{aligned} u &= \frac{-1}{4\pi} \int_0^{2\pi} \frac{d}{d\psi} \left(\frac{d\Gamma}{dL} \right) \frac{2 \sin X \sin^2 \psi}{1 - \sin^2 X \cos^2 \psi} \tan^{-1} \left[\frac{(1 - \sin X \cos \psi) \sqrt{r^2 + x^2 + y^2 + z^2 - 2r(x \cos \psi + y \sin \psi) - r}}{(y \cos \psi - x \sin \psi) \cos X - x \sin X \sin \psi} \right] \\ &\quad - \frac{\sin X \cos X \sin \psi \cos \psi}{1 - \sin^2 X \cos^2 \psi} \ln \left| \frac{\sqrt{r^2 + x^2 + y^2 + z^2 - 2r(x \cos \psi + y \sin \psi) + (z \cos X - x \sin X) + r} \sin X \cos \psi}{\sqrt{r^2 + x^2 + y^2 + z^2 - 2r(x \cos \psi + y \sin \psi) - (z \cos X - x \sin X) + r} \sin X \cos \psi} \right| \\ &\quad - \frac{\cos X \sin \psi}{1 - \sin^2 X \cos^2 \psi} \ln 2 \left| \frac{r - (x \cos \psi + y \sin \psi) - \sqrt{r^2 + x^2 + y^2 + z^2 - 2r(x \cos \psi + y \sin \psi)}}{r - (x \cos \psi + y \sin \psi) + \sqrt{r^2 + x^2 + y^2 + z^2 - 2r(x \cos \psi + y \sin \psi)}} \right| \Bigg|_0^R. \end{aligned} \quad (25)$$

Equation (25), after substituting limits and nondimensionalizing becomes

$$\frac{u}{w_0} = \frac{1}{2\pi} \int_0^{2\pi} \frac{df(\psi)}{d\psi} \left\{ \frac{2 \sin X \sin^2 \psi}{1 - \sin^2 X \cos^2 \psi} \left\langle \tan^{-1} \left[\frac{(1 - \sin X \cos \psi)(R_c' - 1) + A + B}{C} \right] - \tan^{-1} \left[\frac{(1 - \sin X \cos \psi)R_0' + A + B}{C} \right] \right\rangle \right\}$$

$$- \frac{\sin X \cos X \sin \psi \cos \psi}{1 - \sin^2 X \cos^2 \psi} \ln \left| \frac{R_c' + B + \sin X \cos \psi}{R_0' + B} \right| - \frac{\cos X \sin \psi}{1 - \sin^2 X \cos^2 \psi} \ln \left| \frac{R_c' + A - 1}{R_0' + A} \right| \right\}, \quad (26)$$

or when the inverse tangent terms are combined as before

$$\frac{u}{w_0} = \frac{1}{2\pi} \int_0^{2\pi} \frac{df(\psi)}{d\psi} \left\{ \frac{2 \sin X \sin^2 \psi}{1 - \sin^2 X \cos^2 \psi} \tan^{-1} \left[\frac{C(R_c' - R_0' - 1)(1 - \sin X \cos \psi)}{R_0'(R_c' - 1)(1 - \sin X \cos \psi)^2 + (A + B)(R_c' + R_0' - 1)(1 - \sin X \cos \psi) + (A + B)^2 C^2} \right] \right.$$

$$\left. - \frac{\sin X \cos X \sin \psi \cos \psi}{1 - \sin^2 X \cos^2 \psi} \ln \left| \frac{R_c' + B + \sin X \cos \psi}{R_0' + B} \right| - \frac{\cos X \sin \psi}{1 - \sin^2 X \cos^2 \psi} \ln \left| \frac{R_c' + A - 1}{R_0' + A} \right| \right\} d\psi. \quad (27)$$

From equation (14), the lateral, or \bar{j} , component of induced velocity is

$$v = \frac{1}{4\pi} \int_0^{2\pi} \int_0^\infty \frac{\frac{d}{d\psi} \left(\frac{dL}{dL} \right) (\cos \psi) (z + L \cos X) dL dr d\psi}{\left[r^2 + x^2 + y^2 + z^2 - 2r(x \cos \psi + y \sin \psi) + 2L(z \cos X - x \sin X + r \sin X \cos \psi) + L^2 \right]^{\frac{3}{2}}}. \quad (28)$$

Noting that equation (28) differs from equation (23) only by a factor of $-\cot \psi$, which does not enter into the first two integrations, the expressions for the lateral component of velocity ratio can be written immediately from equations (26) and (27) as

$$\frac{v}{w_0} = \frac{-1}{2\pi} \int_0^{2\pi} \frac{df(\psi)}{d\psi} \left[\frac{2 \sin X \sin \psi \cos \psi}{1 - \sin^2 X \cos^2 \psi} \tan^{-1} \left[\frac{(1 - \sin X \cos \psi)(R_C' - 1) + A + B}{C} \right] \right] - \tan^{-1} \left[\frac{(1 - \sin X \cos \psi)R_C' + A + B}{C} \right] d\psi,$$

$$- \frac{\sin X \cos X \cos^2 \psi}{1 - \sin^2 X \cos^2 \psi} \ln \left| \frac{R_C' + B + \sin X \cos \psi}{R_0' + B} \right| - \frac{\cos X \cos \psi}{1 - \sin^2 X \cos^2 \psi} \ln \left| \frac{R_C' + A - 1}{R_0' + A} \right| d\psi, \quad (29)$$

or

$$\frac{v}{w_0} = \frac{-1}{2\pi} \int_0^{2\pi} \frac{df(\psi)}{d\psi} \left[\frac{2 \sin X \sin \psi \cos \psi}{1 - \sin^2 X \cos^2 \psi} \tan^{-1} \left[\frac{C(R_C' - R_0' - 1)(1 - \sin X \cos \psi)}{R_0'(R_C' - 1)(1 - \sin X \cos \psi)^2 + (A + B)(R_C' + R_0' - 1)(1 - \sin X \cos \psi) + (A + B)^2 + C^2} \right] \right] - \frac{\sin X \cos X \cos^2 \psi}{1 - \sin^2 X \cos^2 \psi} \ln \left| \frac{R_C' + B + \sin X \cos \psi}{R_0' + B} \right| - \frac{\cos X \cos \psi}{1 - \sin^2 X \cos^2 \psi} \ln \left| \frac{R_C' + A - 1}{R_0' + A} \right| d\psi. \quad (30)$$

Numerical calculations. - The preceding sections of this thesis have presented expressions for the induced velocities in terms of integrals. Unfortunately, these integrals are not, in general, expressible in terms of elementary functions (ref. 3). Therefore, numerical integration is necessary to obtain usable results. The complexity of these expressions (eqs. (9), (11), (13), (2), (27), and (30)) makes manual computation uneconomical; therefore, the equations were coded for integration on the IBM 704 automatic digital computer located at the Langley Laboratory of the NACA.

Trial calculations were made first in order to determine the accuracy of the computing program. The location of the point P was confined to the lateral axis within the rotor disk, and a unit vortex density was chosen. For this case, Katzoff (ref. 11) has shown that the induced-velocity ratio is always unity. Simpson's rule with an interval of three degrees, when used with eight significant figures (floating decimal system), reproduced this value within 0.0002 except when the point was less than three percent of the radius from the edge of the rotor disk. This procedure was selected for the ensuing calculations on the assumption that it would yield reasonable accuracy at other locations and for other vorticity distributions.

In order to hold the machine time to a reasonable total, only the normal component of induced velocity was computed. This should not be a severe restriction since the normal component is, in general, the component of major interest.

Three skew angles, $\chi = \tan^{-1} 2$, $\tan^{-1} 4$, and $\tan^{-1} 10$, were selected. This range of skew angles encompasses virtually all forward-flight conditions for the helicopter, and a large portion of the transition speed range for convertiplanes.

The capacity of the computing machine was such that calculations could be made simultaneously for two different vorticity distributions. These were chosen as $f(\psi) = 1$ and $f(\psi) = \sin \psi$. It will be shown in a succeeding section that these two vorticity distributions are sufficient for a reasonable representation of the rotor.

Certain locations in the vicinity of the rotor present more interesting fields of research than others. One of these is the longitudinal plane where the fuselage and tail are located. Symmetry (ref. 5) shows, however, that possible tip-speed ratio effects are small in this plane so that available calculations (refs. 8 and 11) should be adequate for most purposes. Experimentally (ref. 11), the lateral rotor plane has been shown to experience large side-to-side asymmetries due to forward speed. Since, in general, this will be the location of the wings on a convertiplane, a knowledge of the flow in this region is of interest for performance calculations. The calculations were therefore confined to the lateral plane.

Since there appeared to be some possibility that the induced velocity of the inner wake might be of small magnitude, the first calculations were programmed to print out the individual contribution of each part of the wake. The results of these calculations are presented in figure 2, where it is evident that the induced velocity contributions of both parts of the wake are of the same order of magnitude. For the

remainder of the calculations only the sum, the total induced velocity, was printed out.

The final computing program was such that the total induced velocity for both vorticity distributions was calculated at a rate of 3 to 4 seconds per point in space.

The calculated velocities for the $\sin \psi$ component of vorticity are presented in tables II to IV, and also in the form of contour charts in figures 3 and 4. The calculated velocities for the constant vorticity case check almost exactly those given in reference 8, and consequently are not presented herein.

Vorticity distribution of the rotor. - The remaining task is to relate the circulation in the wake and on the rotor blades to the thrust of the rotor. Consider a helicopter rotor in forward flight. The velocity of any blade element is (ref. 1)

$$U = \Omega R \left(\frac{r}{R} + u \sin \psi \right). \quad (31)$$

The lift due to the blade element will then be

$$dL = \rho \Omega R \left(\frac{r}{R} + u \sin \psi \right) \Gamma dr, \quad (32)$$

where it is understood that Γ is a function both of radial position and of azimuth angle and the entire thrust is considered to be concentrated on a single representative blade. The rotor thrust is found by integrating equation (32) along the blade and averaging with respect to azimuth angle to give

$$T = \frac{\rho \Omega R}{2\pi} \int_0^{2\pi} \int_0^R \left(\frac{r}{R} + \mu \sin \psi \right) \Gamma dr d\psi. \quad (33)$$

In order to accomplish the integrations of equation (33) it is necessary to know Γ as a function of r and ψ . If the loading is relatively constant with azimuth position, it is evident that the circulation must have a large sinusoidal component. Furthermore, since the loading must be zero at the center of the rotor, the circulation should also be zero at the center. For the present purpose, the circulation is taken as

$$\Gamma = \Gamma_0 \left[\left(\frac{r}{R} \right)^n - \mu \left(\frac{r}{R} \right)^{n-1} \sin \psi \right], \quad (34)$$

where Γ_0 and n are constants. The assumption that the sinusoidal portion of the circulation varies radially as $1/r$ times the constant part of the circulation is purely arbitrary. However, it will be shown now that this assumption does meet additional requirements and that it also entails certain simplifications in the analysis.

Substituting equation (34) into equation (32) yields

$$dL = \rho \Omega R T_0 \left[\left(\frac{r}{R} \right)^{n+1} - \frac{\mu^2}{n} \left(\frac{r}{R} \right)^{n-1} + \frac{\mu^2}{n} \left(\frac{r}{R} \right)^{n-1} \cos 2\psi \right] dr. \quad (35)$$

Thus the blade-element loading will have no first harmonic component if the circulation is as assumed herein. Furthermore, the thrust moment of the blade about the flapping pin will also have no first harmonic. This result is in agreement with blade-element theory (for

example, ref. 15) which indicates that the first harmonic thrust moment is indeed small. The second harmonic component of the blade-element thrust as given by equation (55) has been checked numerically for several flight conditions and is appreciably smaller than that indicated by blade-element theory. Thus the rotor of the present analysis may be considered as having nearly constant azimuthwise loading.

Now substitute equation (54) into equation (33) and integrate to obtain

$$T = \rho \Omega R^2 \left(\frac{1}{n+2} - \frac{\mu^2}{2n} \right) \quad (36)$$

where n is neither 0 nor -2.

Substitute for Γ_0 from equation (36) in equation (34) to determine the value of the circulation over the rotor disk, which is

$$\Gamma = \frac{T}{\rho \Omega R^2 \left(\frac{1}{n+2} - \frac{\mu^2}{2n} \right)} \left[\left(\frac{r}{R} \right)^n - \mu \left(\frac{r}{R} \right)^{n-1} \sin \psi \right]. \quad (37)$$

Equations (36) and (37) are sufficient to relate the thrust to the wake vorticity for an arbitrary radial distribution of load. The analysis is, however, much simpler if restricted to a triangular loading ($n = 1$). Since the assumptions of an undeformed wake and an approximately axisymmetric loading greatly restrict the maximum accuracy of the analysis, and since the actual rotor loading is not at present calculable (ref. 16), the assumption of triangular loading is probably satisfactory. For this case equations (36) and (37) become

$$T = \frac{\rho \Omega R^2}{3} \left(1 - \frac{3}{2} \mu^2 \right); \quad (38)$$

$$\Gamma = \frac{3T}{\rho \Omega R^2 \left(1 - \frac{3}{2} \mu^2 \right)} \left[\frac{r}{R} - \mu \sin \psi \right]. \quad (39)$$

Consider first the portion of the circulation which is constant with respect to azimuth position. This part represents an axisymmetric loading in the sense of reference 11. For the triangularly loaded rotor case of reference 11, where $\mu = 0$,

$$\Gamma = \frac{3T}{\rho \Omega R^2} \frac{r}{R}. \quad (40)$$

Thus the induced velocities contributed by the constant part of the vorticity may be obtained from the results of reference 11 merely by multiplying the induced velocities given therein by $\frac{1}{1 - \frac{3}{2} \mu^2}$. In order to facilitate the work, charts similar to these of reference 11 have been computed for the lateral plane from the results of reference 8. These charts are presented in figure 5.

The sinusoidal component of equation (39) is uniform along the radius and its value for unit strength may be read directly from figures 3 and 4 of this thesis. Since the loading is assumed triangular, the constant of $3/2$ from reference 11 must be inserted in this portion of the calculation as well. The values from figures 3 and 4 must

therefore be multiplied by $\frac{-\frac{3}{2}}{1 - \frac{3}{2}r^2}$. The total induced velocity at P

is then

$$\frac{w}{w_0} = \frac{1}{1 - \frac{3}{2}r^2} \left(\frac{w}{w_0} \text{ from fig. 5} \right) + \frac{\frac{3}{2}}{1 - \frac{3}{2}r^2} \left(\frac{w}{w_0} \text{ from fig. 3} \right). \quad (41)$$

It will be noted that figures 2 to 5 present induced velocity contours for only the advancing side of the rotor. These values may be inserted directly into equation (41) when dealing with the advancing side of the rotor. The flow-field possesses certain symmetries which are noted on the figures. Thus the flow over the retreating half of the disk is identical to that of the advancing half when the vorticity is constant with respect to azimuth angle. The sinusoidal vorticity, however, results in an antisymmetric velocity field, and consequently, the induced velocity ratios of figures 2 to 4 must be multiplied by -1 when used for the retreating side of the disk.

IV. DISCUSSION OF CALCULATED RESULTS

The most striking feature of the calculated flow (figs. 3 and 4) is the extent to which the effect of sinusoidal vorticity is concentrated near the tips of the rotor. This is in marked contrast to the flow generated by a uniform vorticity (ref. 8) where the induced velocity gradient across the wake is relatively mild. This result might have been anticipated since in the present case the vorticity is not only greatest near the rotor tips, but it also changes sign from one side of the rotor to the other.

It is also evident that the effect of sinusoidal vorticity dies out rapidly with distance from the rotor. The reason for this is apparent from figure 2 which indicates that the effects of the inner and outer wakes counteract each other at locations greater than one radius from the center, whereas they tend to add at locations near the rotor.

The only previous attempt to compute the asymmetry of flow due to forward speed is that of Drees (ref. 5). He assumed that the sinusoidal portion of the vortex system could be represented by two smaller cylindrical vortex sheets similar to, but disposed laterally within, the original cylindrical sheet representing the outer wake. The induced velocity contribution at the three-quarter radius point of the lateral axis was found by numerical integration to be $\frac{w}{w_0} = -\frac{3}{2}\mu$ (based, however,

on a w_0 which already includes the $\frac{1}{1 - \frac{3}{2}\mu^2}$ factor found in the

previous section). It has since become evident from Katzoff's symmetry

theorems (ref. 11) that this system produces a uniform induced velocity across each side of the rotor; however, at that time it was suggested that this result indicated a linear lateral distribution of induced velocity with a slope of $-2u$.

Figure 6 compares the present results with those of reference 5. Surprisingly enough, the results are closely similar at the three-quarter radius over a large range of tip-speed ratios (fig. 6(a)). When the induced velocity distribution is considered, however, the results may be less satisfactory. This is shown for a tip-speed ratio of 0.30 in figure 6(b). The difference is even greater if the actual induced velocity of the vortex system of reference 5 is considered.

V. COMPARISON WITH EXPERIMENT

Although the induced-velocity equations were derived with no restrictions as to location in space, a comparison with experiment is restricted to the lateral plane of the rotor by the limited extent of the numerical calculations. The only extensive experimental investigation of this region is that of reference 11. Before actually comparing the calculated and measured induced velocities, certain shortcomings of the investigation of reference 11, and of the present thesis, should be noted and borne in mind. First the accuracy of the flow surveys ranged from 10 to 15 percent of the mean induced velocity depending upon the particular flight condition. Furthermore, the measurements indicate that the flow in the lateral plane is particularly sensitive to the actual detailed rotor load distribution. The present analysis, as previously noted, has assumed a very nearly symmetric triangular loading, which is not actually the case as has been shown by reference 16. Therefore, some discrepancy, particularly at the edges of the rotor, would be expected in the following comparison.

Figure 7(a) compares calculated and measured induced velocities for a low-speed level-flight ($U = 0.075$) helicopter condition. Since the forward speed is so low, there should be little difference from side to side on the rotor. This is verified both by the theory and by the experimental measurements. In general, however, the correct trend is indicated by the theory. (See particularly $z = -0.07$.) The error is fairly large near the outer part of the wake below the rotor ($z = -0.14$ and -0.10). This discrepancy is partially due to differences between

the assumed and actual disk loadings (see fig. 10 of ref. 16). However, the error is probably more directly chargeable to the rapid roll-up of the lower part of the wake, which has already been carried back a full radius from the leading edge of the rotor disk.

Figure 7(b) presents a similar comparison at a tip-speed ratio of 0.140 which represents a cruising flight condition for a helicopter. In general, the new theory represents an improvement in accuracy over the older symmetrical vorticity calculations. The effect of variances from the assumed triangular load distribution is shown at the vertical locations closest to the rotor. The effects of wake roll-up are less in this case because of the lower lift coefficient, and consequently the calculated induced velocities are much closer to the measured velocities even near the lower edge of the wake.

A noticeable departure from the trend of reasonable agreement is shown outside the retreating tip of the rotor. Here the new theory indicates a considerably increased upwash over that predicted by the older theory. This is not borne out by the measurements, which indicate the same, or even less, upwash here than on the advancing side of the rotor. The reasons for this variance are not understood at present, but may be a matter of some concern. References 10 and 17 indicate that the mean induced velocities may be used in estimating the interference between rotors of multirotor configurations. Since this is so, it would be expected theoretically that the performance of a side-by-side rotor system would be greatest when the blades retreat on the adjacent sides of the rotors. The experimental flow measurements, however, indicate

that the differences due to direction of rotation should be minor, and perhaps even in the opposite sense from that indicated by the theory. Effects such as these provide a fertile field for further investigation, both theoretical and experimental.

Figure 7(c) compares theory and experiment for a fairly high-speed flight condition ($\mu = 0.232$). This particular set of measurements has the least accuracy of those given in reference 11. On the other hand, however, the effects of asymmetry are also the greatest here. The degree of improvement offered by the new theory is evident as well as is the shortcoming of the theory at locations outside the retreating tip.

Figure 8 compares the theoretical velocities with the extrapolated data of reference 11 in the plane of the rotor itself. This figure summarizes most of the previous discussion of figure 7. It also vividly demonstrates the extent to which the load distribution on the rotor changes with tip-speed ratio. If the actual instantaneous induced velocities were known it would, of course, be possible to obtain the loading on the rotor. Unfortunately, present rotor blade-element-theory does not yield adequate results when used to calculate the blade load distribution (ref. 16). Its failure in this regard is primarily a result of assuming that the inflow is uniform over the entire rotor. Other sources of error, such as the usual small angle assumptions and sharply cut-off tip losses, are apparent but are probably of a smaller magnitude. It might be thought, at first glance, that the insertion of the local values of the mean induced velocities in the appropriate

places in blade-element-theory would greatly improve the accuracy of the analysis. In this regard it is well to consider some of the results of reference 13.

Reference 13 is an experimental investigation of the induced velocities in the plane of a rotor. The induced velocities were obtained by measuring the instantaneous pressure distribution on a rotor blade by means of pressure cells, and then working backward through the blade-element theory to obtain the induced velocity required to produce the measured loading. The results, of course, include all the errors inherent in the theory, but at least it may be said that these induced velocities are the velocities which will give the observed loading.

The data points shown on figure 9 correspond to one flight condition of reference 13. The solid curve represents the mean induced velocity calculated on the basis of our present knowledge. It is immediately evident that there is no correlation at all between the measured and calculated results. Even the trends of the curves are completely reversed over the front half of the longitudinal centerline. Similar results may be obtained from the loadings of reference 16 where the pressure gages, having much faster response, may be considered more accurate.

Figure 9 is in direct contrast to the reasonable agreement shown previously in figures 7 and 8, and may be explained as follows: The actual wake vortices are approximately skewed spirals emanating from the rotor blade. Thus their location in space, and consequently the velocities induced by them, will be distinct functions of the blade azimuth position. This relationship between blade azimuth position and induced

velocity was lost when the wake vorticity was assumed to be uniformly distributed. The nonuniformity of vorticity has little or no effect on the time-averaged reading of a survey probe (such as that of ref. 11) fixed at a point in space, however, the rotating blade, being tied, so to speak, to the vortex system, sees some induced velocity other than the mean value. Thus, the induced velocities given by the present report should not be used for detailed blade loading studies.

Two recent papers (references 18 and 19) have indicated that the blade loading problem is actually analogous to the flutter problem of fixed-wing aircraft. Using flutter theory, but modifying the wake vortex pattern to more nearly correspond with that of a rotor, these investigations have shown that the unsteady aerodynamics of the blade plays a large part in determining the loading. It would seem likely, therefore, that this approach is more appropriate to the blade load problem than are attempts to combine the present results with blade-element theory.

VI. CONCLUSIONS

The following results have been obtained from this theoretical study of the effect of tip-speed ratio and the associated asymmetry of flow on the induced velocities in the vicinity of a lifting rotor:

1. Equations, suitable for numerical integration, have been developed for the three components of induced velocity.
2. Numerical results, in the form of charts and tables, have been presented for the normal induced velocity in the lateral plane of a rotor having a $\sin \psi$ vorticity distribution.
3. Charts of the normal induced velocity in the lateral plane of a rotor having a symmetrical triangular vorticity distribution have been presented.
4. When compared with previously made wind-tunnel flow-measurements, the present results appear to be more accurate than previously available theoretical results.
5. When compared with the induced velocities obtained by previous rotor-blade pressure-distribution measurements, the present results appear to be inapplicable to the calculation of rotor blade loads.

VII. SUMMARY

A theoretical investigation of the asymmetry of induced flow in the vicinity of a lifting rotor in forward flight has been conducted. The analysis is based upon an asymmetric wake which is a logical extension of that used for previous investigations. Equations for the induced velocities at an arbitrary point in space are presented in a form suitable for numerical integration. Numerical results for the normal induced velocity in the lateral plane of the rotor are presented in the form of tables and charts. Comparison with previously available measurements indicates an improvement in accuracy over older theories. The results should be useful in estimating the interference between wing and rotor of compound helicopters and convertiplanes. In addition the results should be applicable to the problem of mutual interference between rotors of multi-rotor helicopters.

VIII. ACKNOWLEDGMENTS

The author wishes to express his appreciation to Dr. S. Katzoff of the NACA who initially suggested the topic of this thesis and who provided guidance and encouragement throughout the course of the investigation. Further, the author's thanks and gratitude are extended to Professor A. C. Bruce of the Virginia Polytechnic Institute for his advice and help during the course of the work, and to Dr. R. W. Truitt for his friendly encouragement throughout the author's studies.

II. BIBLIOGRAPHY

1. Glauert, H.: A General Theory of the Autogiro. R. & M. no. 1111, British A.R.C., Nov. 1926.
2. Wheatley, John B.: An Aerodynamic Analysis of the Autogiro Rotor with a Comparison Between Calculated and Experimental Results. NACA Rep. 487, 1934.
3. Coleman, Robert P., Feingold, Arnold M., and Stempin, Carl W.: Evaluation of the Induced Velocity Field of an Idealized Helicopter Rotor. NACA VR L-146, 1945. (Formerly AER 10810.)
4. Glauert, H.: Airplane Propellers. Helicopter Airscrews. Vol. IV of Aerodynamic Theory, div. L, ch. X, sec. 5, W. F. Durand, ed., Julius Springer (Berlin), 1935, p. 319.
5. Drues, J. Meijer: A Theory of Air Flow Through Rotors and Its Application to Some Helicopter Problems. Jour. Helicopter Assoc. of Great Britain, vol. 3, no. 2, July-Aug.-Sept. 1949, pp. 79-104.
6. Mangler, K. W., and Squire, H. B.: The Induced Velocity Field of a Rotor. R. & M. no. 1642, British A.R.C., May 1950.
7. Castles, Walter, Jr., and DeLeeuw, Jacob Henri: The Normal Component of the Induced Velocity in the Vicinity of a Lifting Rotor and Some Examples of Its Application. NACA Rep. 1184, 1954. (Supersedes NACA TN 2912.)
8. Castles, Walter, Jr., and Durham, Howard L., Jr.: Distribution of Normal Component of Induced Velocity in Lateral Plane of a Lifting Rotor. NACA TN 3841, 1956.
9. Castles, Walter, Jr., Durham, Howard L., Jr., and Kevorkian, Jirair: Normal Component of Induced Velocity for Entire Field of a Uniformly

- Loaded Lifting Rotor with Highly Swept Wake as Determined by Electromagnetic Analogy. NACA TN 4238, 1958.
10. Heyson, Harry H.: Preliminary Results from Flow-Field Measurements Around Single and Tandem Rotors in the Langley Full-Scale Tunnel. NACA TN 3242, 1954.
11. Heyson, Harry H., and Katzoff, S.: Induced Velocities Near Lifting Rotor With Nonuniform Disk Loading. NACA Rep. 1319, 1957.
(Supersedes NACA TN's 3690 and 3691.)
12. Ross, Robert S.: An Investigation of the Air Flow Underneath Helicopter Rotors. Jour. Aero. Sci., vol. 13, no. 12, Dec. 1946, pp. 665-677.
13. Falabella, Gaetano, Jr., and Meyer, John R., Jr.: Determination of Inflow Distributions From Experimental Aerodynamic Loading and Blade-Motion Data on a Model Helicopter Rotor in Hovering and Forward Flight. NACA TN 3492, 1955.
14. Peirce, B. O.: A Short Table of Integrals. Third rev. ed., Ginn and Co., 1929, pp. 10, 24, 34, 80.
15. Gessow, Alfred, and Myers, Garry C., Jr.: Aerodynamics of the Helicopter. Macmillan Co., 1952, p. 193.
16. Rabbott, John P., Jr., and Churchill, Gary B.: Experimental Investigation of the Aerodynamic Loading on a Helicopter Rotor Blade in Forward Flight. NACA RM L56I07, 1956.
17. Dingeldein, Richard C.: Wind-Tunnel Studies of the Performance of Multirotor Configurations. NACA TN 3236, 1954.

18. Timman, R., and van de Vooren, A. L.: Flutter of a Helicopter Rotor Rotating in Its Own Wake. *Jour. Aero. Sci.*, vol. 24, no. 9, Sept. 1957, pp. 694-702.
19. Loewy, R. G.: A Two-Dimensional Approximation to the Unsteady Aerodynamics of Rotary Wings. *Jour. Aero. Sci.*, vol. 24, no. 2, Feb. 1957, pp. 81-92, 144.

Most of the recent literature on the subject of rotor flow fields is included in the above list. The reader's attention is particularly directed to references 5, 5, 7, 8, 11, and 12. Two additional papers which summarize most of the work in the field previous to 1954 and 1956, respectively, are:

Gessow, Alfred: Review of Information on Induced Flow of a Lifting Rotor. NACA TN 3238, 1954.

Payne, P. R.: Induced Aerodynamics of Helicopters. Part I, Feb. 1956, pp. 46-51, 54; Part II, March 1956, pp. 82-87; Part III, April 1956, pp. 123-129; Part IV, May 1956, pp. 148-153, *Aircraft Engineering*.

X. VITA

The author was born in Far Rockaway, New York, on November 7, 1925. He attended public school in New York City and graduated from Brooklyn Technical High School in 1943. After an interruption for service in the United States Army Air Force, he resumed his studies at the Polytechnic Institute of Brooklyn where he received the degree of Bachelor of Aeronautical Engineering, cum laude, in 1949. His bachelor's thesis was entitled, "A Theoretical Investigation of Suction Airfoils."

Following graduation, he accepted a position as an Aeronautical Research Engineer at the Langley Laboratory of the National Advisory Committee for Aeronautics. His work has been concerned with the performance and induced aerodynamics of helicopters, and he is the author of several reports on these subjects.

Harry H. Heyson

III. ANALYSIS

EVALUATION OF CERTAIN INTEGRALS OCCURRING IN THE ANALYSIS

The analysis of the inner wake involves integrals of the forms:

$$\int \frac{dx}{x + (cx + d)\sqrt{x}} \quad \text{and} \quad \int \frac{dx}{\sqrt{x + cx + d}},$$

where $M = a + bx + x^2$.

Both forms may be evaluated by use of the substitution (item 35, ref. 14)

$$u = \sqrt{x} + x$$

The first form is the simpler of the two and will be evaluated first. The indicated substitution reduces this form to

$$\int \frac{dx}{x + (cx + d)\sqrt{x}} = \int \frac{du}{(c - 1)u^2 + (b - cd)u + (db - a - ac)}. \quad (A1)$$

The right hand side of equation (A1) may be integrated by item 67 of reference 14 to yield

$$\int \frac{dx}{x + (cx + d)\sqrt{x}} = \frac{4}{\sqrt{q}} \tan^{-1} \left[\frac{2(c - 1)u + b - 2d}{\sqrt{q}} \right], \quad (A2)$$

where $q = 4db(c - 1) + 4a(1 - c^2) - (b - cd)^2$.

The final expression is obtained by returning equation (A2) to the original variable, x .

$$\int \frac{dx}{x + (cx + d)\sqrt{x}} = \frac{4}{\sqrt{q}} \tan^{-1} \left[\frac{c(c-1)(\sqrt{x} - x) + b - ad}{\sqrt{q}} \right], \quad (3)$$

where q is as given above.

Evaluation of the second form is a more lengthy task, but proceeds in the same manner. Making the same substitution as before yields

$$\int \frac{dx}{\sqrt{x} + cx + d} = \int \frac{2(bu - a - u^2)du}{(b + cu)[(c - 1)u^2 + (b - d)u + (db - a - ac)]}. \quad (4)$$

Now separate the right hand side of equation (4) into partial fractions to obtain

$$\begin{aligned} \int \frac{dx}{\sqrt{x} + cx + d} &= \frac{1}{1 + c} \int \frac{2 du}{b + cu} \\ &+ \frac{ac}{1 + c} \int \frac{u du}{[u^2(c - 1) + u(b - d) + (db - a - ac)]} \\ &- \frac{a}{1 + c} \int \frac{du}{[u^2(c - 1) + u(b - d) + (db - a - ac)]}. \end{aligned} \quad (4)$$

The first term may be integrated by inspection, and the second term may be integrated by item 72 of reference 14 to give

$$\begin{aligned} \int \frac{dx}{\sqrt{x+cx+d}} &= \frac{-1}{1+c} \ln(b+cu) \\ &+ \frac{c}{c^2-1} \ln \left[u^2(c-1) + u(b+ad) + (db-a+ac) \right] \\ &- \frac{bc-ad}{c^2-1} \int \frac{du}{u^2(c-1) + u(b+ad) + (db-a+ac)}. \end{aligned} \quad (46)$$

The remaining integral may be evaluated by means of item 67 of reference 14 to yield

$$\begin{aligned} \int \frac{dx}{\sqrt{x+cx+d}} &= \frac{-1}{1+c} \ln(b+cu) \\ &+ \frac{c}{c^2-1} \ln \left[u^2(c-1) + u(b+ad) + (db-a+ac) \right] \\ &- \frac{bc-ad}{c^2-1} \frac{2}{\sqrt{1}} \tan^{-1} \left[\frac{2(c-1)u+b+d}{\sqrt{1}} \right], \end{aligned} \quad (47)$$

where q has the same meaning as in equations (40) and (43).

Now return equation (47) to the original variable x , resulting in

$$\begin{aligned} \int \frac{dx}{x+cx+d} &= \frac{-c-1}{c^2-1} \ln \left[b+\sqrt{x}+c\sqrt{1} \right] \\ &+ \frac{c}{c^2-1} \ln \left[(\sqrt{x}-x)^2(c-1) \right. \\ &\quad \left. + (\sqrt{x}-x)(b+ad) + (db-a+ac) \right] \\ &- \frac{bc-ad}{c^2-1} \frac{2}{\sqrt{1}} \tan^{-1} \left[\frac{(c-1)(\sqrt{x}-x)+b+d}{\sqrt{1}} \right]. \end{aligned} \quad (48)$$

Note that

$$\begin{aligned} &(\sqrt{x}-x)^2(c-1) + (\sqrt{x}-x)(b+ad) + (db-a+ac) \\ &= (b+cx-\sqrt{x})(\sqrt{x}+cx+d), \end{aligned}$$

so that the logarithmic terms of equation (48) may be combined to yield

$$\begin{aligned} \int \frac{dx}{\sqrt{x+cx+d}} &= \frac{c}{c^2-1} \ln[\sqrt{c+x+d}] + \frac{1}{c^2-1} \ln[b+x-2\sqrt{c}] \\ &\quad - \frac{bc+ad}{c^2-1} \frac{2}{\sqrt{c}} \tan^{-1} \left[\frac{2(c-1)(x-b)+2d}{\sqrt{c}} \right]. \end{aligned} \quad (49)$$

The presence of the logarithmic terms in equation (49) occasions imaginary values for the integral if either $(\sqrt{x+cx+d})$ or $(b+x-2\sqrt{c})$ is negative. Provided that these terms are monotonically negative, this result may be avoided as follows:

Write equation (49) as

$$\begin{aligned} \int \frac{dx}{\sqrt{x+cx+d}} &= \frac{1}{1+c} \int \frac{du}{u-b} \\ &\quad - \frac{c}{1+c} \int \frac{u du}{[u^2(1+c)+u(b-d)+(db-a-ac)]} \\ &\quad - \frac{ad}{1+c} \int \frac{du}{[u^2(c-1)+u(b-d)+(db-a-ac)]}. \end{aligned} \quad (50)$$

Integration, as before, of the first two terms results in

$$\begin{aligned} \int \frac{dx}{\sqrt{x+cx+d}} &= \frac{1}{1+c} \ln(2u-b) \\ &\quad + \frac{c}{c^2-1} \ln[u^2(1+c)+u(db-a-ac)+(db-a-ac)] \\ &\quad - \frac{bc+ad}{c^2-1} \int \frac{du}{[u^2(c-1)+u(c-a)+db-a-ac]}. \end{aligned} \quad (51)$$

Comparison of equations (6) and (11) indicates that the only difference is a reversal in sign of the arguments of the logarithmic terms. Therefore, as long as these arguments are monotonically either positive or negative, the final expression may be written as

$$\begin{aligned} \int \frac{dx}{\sqrt{x+cx+d}} &= \frac{c}{c^2-1} \ln \left| \sqrt{x+cx+d} \right| + \frac{1}{c^2-1} \ln \left| b+2x-2\sqrt{x} \right| \\ &\quad - \frac{bc+2d}{c^2-1} \frac{2}{\sqrt{q}} \tan^{-1} \left[\frac{2(c-1)(\sqrt{x}-x) + b+2d}{\sqrt{q}} \right], \end{aligned} \quad (A12)$$

where, again, $q = 4db(c-1) + 4a(1-c^2) \approx (b+2d)^2$.

TABLE I
LIMITING VALUES OF ARC TANGENT IN EQUATION 22

Location of P	Azimuth angle, ψ		Arc tangent
	degrees	radians	
$y = z = 0$	0	$\pm \frac{\pi}{2}$	
	180	0	
$x = z = 0$	90	$\pm \frac{\pi}{2}$	
	270	0	

TABLE III.
 CALCULATED VALUES OF INDUCED-VELOCITY RATIO, w/w_0 , IN THE LATERAL PLANE
 OF A ROTOR WITH UNIT SINE Ψ VORTICITY, $\chi = \tan^{-1} 2 = 63.43^\circ$.

y'	Values of w/w_0 for $z' = 0$														
	0	0.1	0.2	0.3	0.4	0.5	0.6	0.7	0.8	0.85	0.9	0.95	1.0	1.05	1.1
0	0	0	0	0	0	0	0	0	0	0	0	0	0	0	0
.1	.2711	.3027	.3014	.2079	.1467	.1047	.0750	.0537	.0385	.0201	.0169	.0119	.0100	.0083	.0069
.2	.3651	.4522	.3856	.2778	.2002	.1442	.1037	.0743	.0530	.0446	.0271	.0227	.0190	.0158	.0130
.3	.4747	.5146	.4390	.3237	.2361	.1711	.1233	.0884	.0629	.0529	.0445	.0370	.0306	.0261	.0217
.4	.5688	.5956	.4691	.3474	.2538	.1838	.1323	.0946	.0672	.0564	.0471	.0392	.0325	.0267	.0217
.5	.6634	.5556	.4078	.3226	.2293	.1635	.1165	.0826	.0579	.0481	.0397	.0326	.0264	.0210	.0165
.6	.7319	.5956	.4765	.3485	.2520	.1814	.1300	.0927	.0655	.0547	.0456	.0377	.0310	.0252	.0202
.7	.7929	.8594	.5953	.3899	.2643	.1845	.1307	.0929	.0654	.0572	.0482	.0424	.0362	.0294	.0242
.8	.8900	.9421	.6421	.3329	.2216	.1544	.1097	.0779	.0547	.0374	.0304	.0244	.0191	.0146	.0107
.9	.9172	.9453	.6453	.2557	.1704	.1203	.0863	.0615	.0429	.0288	.0230	.0179	.0135	.0096	.0072
.95	.9409	.2760	.1598	.1131	.0835	.0614	.0441	.0304	.0196	.0151	.0110	.0075	.0044	.0016	.0008
1.0	.0324	.0548	.0460	.0361	.0264	.0176	.0101	.0068	.0059	.0039	.0012	.0011	.0002	.0051	
1.05	.1855	.0428	.0023	.0098	.0113	.0088	.0047	.0005	.0015	.0005	.0052	.0068	.0082	.0096	
1.1	.7436	.2990	.1190	.0513	.0234	.0120	.0082	.0078	.0090	.0098	.0107	.0116	.0125	.0133	.0141
1.15	.6185	.3574	.1703	.0907	.0522	.0333	.0240	.0198	.0182	.0179	.0178	.0179	.0181	.0183	.0186
1.2	.5298	.3407	.2006	.1203	.0762	.0519	.0381	.0310	.0269	.0257	.0247	.0241	.0236	.0232	.0230
1.3	.4130	.3138	.2221	.1548	.1099	.0810	.0624	.0504	.0426	.0398	.0374	.0355	.0339	.0336	.0335
1.4	.3392	.2797	.2189	.1675	.1283	.0999	.0798	.0656	.0556	.0517	.0483	.0455	.0431	.0410	.0391
1.6	.2513	.2239	.1938	.1645	.1384	.1165	.0986	.0844	.0731	.0684	.0652	.0605	.0572	.0542	.0515
1.8	.2008	.1854	.1682	.1504	.1334	.1177	.1036	.0919	.0817	.0772	.0731	.0693	.0626	.0597	.0567
2.0	.1679	.1582	.1472	.1357	.1241	.1129	.1025	.0930	.0845	.0806	.0769	.0735	.0703	.0673	.0645
2.5	.1204	.1162	.1116	.1065	.1013	.0959	.0906	.0854	.0803	.0779	.0755	.0732	.0707	.0682	.0657
3.0	.0947	.0924	.0899	.0871	.0842	.0812	.0781	.0750	.0720	.0704	.0689	.0674	.0659	.0645	.0630
3.5	.0784	.0770	.0754	.0737	.0719	.0700	.0680	.0660	.0640	.0630	.0619	.0609	.0599	.0589	.0579
4.0	.0671	.0661	.0650	.0639	.0626	.0613	.0600	.0586	.0572	.0565	.0557	.0520	.0543	.0536	.0529
4.5	.0588	.0580	.0572	.0564	.0555	.0545	.0536	.0526	.0515	.0510	.0505	.0499	.0494	.0483	.0474
5.0	.0523	.0518	.0511	.0505	.0498	.0491	.0484	.0476	.0464	.0460	.0456	.0456	.0452	.0448	.0444
5.5	.0472	.0467	.0463	.0457	.0452	.0447	.0441	.0435	.0429	.0425	.0422	.0419	.0415	.0413	.0409
6.0	.0430	.0426	.0422	.0418	.0414	.0409	.0405	.0400	.0395	.0393	.0390	.0387	.0385	.0382	.0380

TABLE III.
CONTINUED.

y ¹	Values of $\frac{w}{w_0}$ for z^1 of -											
	1.15	1.2	1.3	1.4	1.5	1.6	1.8	2.0	2.5	3.0	3.5	4.0
0	0	0	0	0	0	0	0	0	0	0	0	0
.1	.0056	.0046	.0029	.0017	.0005	-.0010	-.0012	-.0011	-.0010	0	0	0
.2	.0107	.0087	.0055	.0032	.0003	-.0013	-.0020	-.0015	-.0019	-.0006	-.0006	0
.3	.0146	.0118	.0074	.0042	0	-.0021	-.0012	-.0018	-.0013	-.0014	-.0012	-.0004
.4	.0170	.0136	.0085	.0044	-.0006	-.0016	-.0014	-.0011	-.0013	-.0016	-.0010	-.0009
.5	.0174	.0158	.0060	.0037	-.0016	-.0044	-.0028	-.0051	-.0051	-.0024	-.0017	-.0015
.6	.0160	.0125	.0091	.0057	.0065	-.0022	-.0032	-.0060	-.0074	-.0069	-.0058	-.0049
.7	.0073	.0044	.0044	.0002	-.0036	-.0003	-.0053	-.0071	-.0051	-.0090	-.0068	-.0049
.8	.0042	.0016	-.0025	-.0025	-.0096	-.0094	-.0113	-.0110	-.0110	-.0092	-.0077	-.0048
.9	.0008	-.0014	-.0050	-.0077	-.0099	-.0110	-.0120	-.0114	-.0120	-.0098	-.0082	-.0054
.95	-.0029	-.0047	-.0047	-.0077	-.0126	-.0126	-.0129	-.0130	-.0121	-.0104	-.0087	-.0057
1.0	-.0067	-.0082	-.0105	-.0122	-.0143	-.0151	-.0151	-.0151	-.0129	-.0110	-.0091	-.0064
1.05	-.0107	-.0117	-.0154	-.0146	-.0150	-.0156	-.0164	-.0162	-.0144	-.0121	-.0084	-.0070
1.1	-.0147	-.0154	-.0164	-.0171	-.0178	-.0178	-.0178	-.0173	-.0151	-.0127	-.0105	-.0060
1.15	-.0188	-.0190	-.0194	-.0196	-.0196	-.0196	-.0196	-.0184	-.0151	-.0137	-.0105	-.0051
1.2	-.0228	-.0226	-.0226	-.0224	-.0221	-.0215	-.0206	-.0196	-.0166	-.0138	-.0114	-.0065
1.3	-.0295	-.0296	-.0296	-.0292	-.0271	-.0251	-.0234	-.0218	-.0181	-.0149	-.0123	-.0086
1.4	-.0375	-.0361	-.0357	-.0357	-.0318	-.0286	-.0262	-.0240	-.0196	-.0160	-.0132	-.0092
1.6	-.0491	-.0469	-.0431	-.0431	-.0351	-.0351	-.0313	-.0282	-.0224	-.0182	-.0149	-.0124
1.8	-.0571	-.0546	-.0502	-.0465	-.0404	-.0404	-.0357	-.0320	-.0250	-.0201	-.0165	-.0104
2.0	-.0618	-.0594	-.0549	-.0510	-.0445	-.0445	-.0393	-.0351	-.0273	-.0219	-.0180	-.0137
2.5	-.0647	-.0628	-.0591	-.0557	-.0497	-.0445	-.0417	-.0401	-.0317	-.0256	-.0211	-.0176
3.0	-.0616	-.0602	-.0575	-.0549	-.0501	-.0458	-.0420	-.0340	-.0280	-.0234	-.0197	-.0110
3.5	-.0569	-.0559	-.0539	-.0514	-.0484	-.0450	-.0418	-.0349	-.0293	-.0248	-.0212	-.0126
4.0	-.0521	-.0514	-.0500	-.0485	-.0457	-.0430	-.0405	-.0347	-.0298	-.0256	-.0222	-.0159
4.5	-.0478	-.0472	-.0461	-.0451	-.0425	-.0408	-.0387	-.0359	-.0296	-.0259	-.0227	-.0170
5.0	-.0439	-.0435	-.0418	-.0427	-.0418	-.0401	-.0384	-.0368	-.0328	-.0291	-.0258	-.0177
5.5	-.0406	-.0403	-.0396	-.0389	-.0375	-.0362	-.0348	-.0315	-.0283	-.0255	-.0229	-.0182
6.0	-.0377	-.0374	-.0369	-.0363	-.0352	-.0341	-.0329	-.0301	-.0274	-.0249	-.0226	-.0186

TABLE II.

CONTINUED.

y ¹	Values of π/π_Q for z^1 of -											
	-0.1	-0.2	-0.3	-0.4	-0.5	-0.6	-0.7	-0.8	-0.9	-1.0	-1.05	-1.1
0	0	0	0	0	0	0	0	0	0	0	0	0
.1	.2515	.2682	.3024	.3817	.4065	.1022	.0729	.0520	.0368	.0303	.0258	.0178
.2	.5007	.5744	.5126	.6756	.5754	.1851	.1446	.0960	.0572	.0569	.0475	.0325
.3	.5299	.6446	.7508	.8489	.6103	.2456	.1761	.1055	.0875	.0739	.0615	.0394
.4	.6868	.7792	.8336	.9731	.9436	.2674	.1714	.1358	.1139	.0951	.0654	.0508
.5	.7749	.8878	1.0035	1.1237	.4726	.2437	.1775	.1249	.1042	.0864	.0712	.0417
.6	.8896	1.0345	1.1631	.7722	.3263	.1927	.1355	.0937	.0772	.0630	.0507	.0436
.7	.9900	1.1719	1.2995	.5081	.1461	.1022	.0703	.0461	.0276	.0200	.0133	.0074
.8	1.1419	1.3475	1.9592	.0214	-.0127	-.0080	-.0082	-.0112	-.0151	-.0172	-.0192	.0022
.85	1.2471	1.4613	.5259	.1488	-.0936	-.0641	-.0486	-.0403	-.0388	-.0367	-.0364	-.0229
.9	1.5918	1.4277	.4302	.2602	.1685	.1170	.0873	.0693	.0641	.0596	.0562	-.0363
.95	1.5736	-1.0695	.5666	.3502	.2327	-.1643	-.1229	-.0981	-.0808	-.0749	-.0663	-.0498
1.0	-1.7285	-1.0493	.6372	.4131	.2835	-.2043	-.1544	-.1220	-.1102	-.1006	-.0926	-.0631
1.05	-1.3487	-.2712	-.6536	-.4489	-.3194	-.2359	-.1809	-.1439	-.1300	-.1088	-.1007	-.0938
1.1	-1.0108	-.8528	-.6331	-.4618	-.3417	-.2592	-.2022	-.1624	-.1471	-.1342	-.1233	-.0880
1.15	-.7951	-.7368	-.5932	-.4579	-.3523	-.2746	-.2183	-.1775	-.1615	-.1477	-.1329	-.0991
1.2	-.6528	-.6375	-.5463	-.4531	-.3539	-.2834	-.2297	-.1833	-.1730	-.1588	-.1465	-.1092
1.3	-.4807	-.4914	-.4558	-.3990	-.3336	-.2404	-.2048	-.1883	-.1744	-.1621	-.1511	-.1169
1.4	-.3815	-.3934	-.3824	-.3519	-.3148	-.2732	-.2397	-.2086	-.1849	-.1624	-.1511	-.1182
1.6	-.2719	-.2827	-.2831	-.2744	-.2534	-.2107	-.2207	-.2010	-.1915	-.1824	-.1737	-.1555
1.8	-.2128	-.2203	-.2230	-.2211	-.2151	-.2062	-.1934	-.1836	-.1776	-.1715	-.1656	-.1509
2.0	-.1757	-.1811	-.1840	-.1812	-.1820	-.1777	-.1719	-.1649	-.1611	-.1573	-.1533	-.1359
2.5	-.1239	-.1267	-.1287	-.1299	-.1302	-.1297	-.1284	-.1266	-.1254	-.1241	-.1227	-.1196
3.0	-.0967	-.0984	-.0998	-.1007	-.1013	-.1016	-.1015	-.1010	-.1002	-.0992	-.0977	-.1180
3.5	-.0797	-.0809	-.0818	-.0826	-.0832	-.0836	-.0837	-.0835	-.0835	-.0834	-.0832	-.0979
4.0	-.0680	-.0690	-.0696	-.0702	-.0707	-.0711	-.0713	-.0715	-.0715	-.0715	-.0714	-.0826
4.5	-.0595	-.0601	-.0606	-.0611	-.0615	-.0619	-.0621	-.0623	-.0624	-.0625	-.0625	-.0712
5.0	-.0529	-.0534	-.0538	-.0542	-.0545	-.0548	-.0551	-.0553	-.0554	-.0555	-.0555	-.0555
5.5	-.0476	-.0480	-.0484	-.0487	-.0490	-.0493	-.0495	-.0497	-.0498	-.0499	-.0500	-.0500
6.0	-.0434	-.0437	-.0440	-.0443	-.0445	-.0447	-.0449	-.0451	-.0452	-.0453	-.0454	-.0455

TABLE II.
CONCLUDED.

y^*	-1.15	-1.2	-1.3	-1.4	-1.6	-1.8	-2.0	-2.5	-3.0	-3.5	-4.0	-4.5	-5.0	-5.5	-6.0
0	0	0	0	0	0	0	0	0	0	0	0	0	0	0	0
.1	.0146	.0119	.0076	.0045	.0016	-.0026	-.0033	-.0030	-.0025	-.0021	-.0018	-.0015	-.0013	-.0011	0
.2	.0266	.0216	.0136	.0078	.0035	-.0054	-.0066	-.0060	-.0051	-.0043	-.0036	-.0030	-.0026	-.0022	0
.3	.0359	.0273	.0167	.0089	.0009	-.0061	-.0036	-.0100	-.0070	-.0064	-.0054	-.0045	-.0039	-.0033	0
.4	.0349	.0275	.0158	.0071	.0038	-.0035	-.0123	-.0135	-.0120	-.0102	-.0085	-.0071	-.0060	-.0052	-.0044
.5	.0289	.0218	.0104	.0021	-.0085	-.0140	-.0165	-.0171	-.0150	-.0127	-.0106	-.0089	-.0075	-.0064	-.0055
.6	.0162	.0103	.0008	-.0062	-.0151	-.0195	-.0213	-.0201	-.0181	-.0152	-.0127	-.0106	-.0090	-.0077	-.0066
.7	-.0023	-.0261	-.0126	-.0173	-.0232	-.0259	-.0267	-.0247	-.0211	-.0177	-.0147	-.0124	-.0105	-.0089	-.0077
.8	-.0346	-.0365	-.0367	-.0372	-.0304	-.0226	-.0331	-.0325	-.0287	-.0242	-.0201	-.0168	-.0141	-.0119	-.0102
.85	-.0365	-.0365	-.0367	-.0372	-.0375	-.0376	-.0368	-.0355	-.0307	-.0277	-.0213	-.0177	-.0149	-.0126	-.0088
.9	-.0485	-.0475	-.0459	-.0447	-.0417	-.0427	-.0407	-.0385	-.0327	-.0272	-.0225	-.0187	-.0157	-.0133	-.0108
.95	-.0604	-.0582	-.0547	-.0520	-.0479	-.0446	-.0416	-.0347	-.0287	-.0237	-.0197	-.0165	-.0140	-.0120	-.0103
1.0	-.0720	-.0687	-.0633	-.0592	-.0531	-.0485	-.0447	-.0367	-.0302	-.0249	-.0207	-.0173	-.0147	-.0126	-.0108
1.05	-.0830	-.0787	-.0716	-.0662	-.0582	-.0524	-.0478	-.0437	-.0316	-.0260	-.0216	-.0181	-.0154	-.0131	-.0113
1.1	-.0932	-.0881	-.0796	-.0729	-.0632	-.0562	-.0508	-.0406	-.0331	-.0272	-.0226	-.0189	-.0160	-.0137	-.0118
1.15	-.1026	-.0967	-.0870	-.0793	-.0680	-.0600	-.0538	-.0426	-.0345	-.0283	-.0235	-.0197	-.0167	-.0143	-.0123
1.2	-.1109	-.1046	-.0939	-.0853	-.0726	-.0656	-.0562	-.0444	-.0359	-.0294	-.0244	-.0205	-.0174	-.0149	-.0128
1.3	-.1247	-.1176	-.1056	-.0958	-.0810	-.0703	-.0622	-.0510	-.0386	-.0316	-.0262	-.0220	-.0186	-.0160	-.0138
1.4	-.1345	-.1272	-.1147	-.1043	-.0881	-.0763	-.0672	-.0515	-.0412	-.0336	-.0279	-.0234	-.0199	-.0171	-.0148
1.6	-.1435	-.1371	-.1254	-.1152	-.0985	-.0856	-.0754	-.0576	-.0459	-.0375	-.0311	-.0262	-.0223	-.0191	-.0166
1.8	-.1430	-.1378	-.1281	-.1192	-.1039	-.0914	-.0811	-.0625	-.0499	-.0408	-.0340	-.0287	-.0245	-.0211	-.0183
2.0	-.1372	-.1333	-.1257	-.1185	-.1054	-.0941	-.0845	-.0660	-.0531	-.0437	-.0366	-.0310	-.0265	-.0229	-.0199
2.5	-.1162	-.1145	-.1108	-.1070	-.0944	-.0920	-.0851	-.0700	-.0581	-.0488	-.0414	-.0355	-.0307	-.0268	-.0235
3.0	-.0971	-.0963	-.0946	-.0927	-.0868	-.0842	-.0797	-.0689	-.0592	-.0510	-.0442	-.0385	-.0337	-.0297	-.0263
3.5	-.0823	-.0820	-.0811	-.0802	-.0780	-.0751	-.0726	-.0652	-.0579	-.0512	-.0452	-.0400	-.0355	-.0316	-.0283
4.0	-.0711	-.0709	-.0705	-.0700	-.0688	-.0673	-.0656	-.0606	-.0553	-.0500	-.0450	-.0405	-.0364	-.0328	-.0296
4.5	-.0624	-.0623	-.0622	-.0619	-.0613	-.0604	-.0593	-.0560	-.0521	-.0480	-.0440	-.0402	-.0366	-.0334	-.0304
5.0	-.0555	-.0555	-.0554	-.0550	-.0545	-.0545	-.0538	-.0516	-.0488	-.0457	-.0425	-.0393	-.0362	-.0334	-.0307
5.5	-.0500	-.0500	-.0500	-.0500	-.0498	-.0495	-.0491	-.0476	-.0456	-.0432	-.0407	-.0381	-.0355	-.0330	-.0306
6.0	-.0455	-.0455	-.0456	-.0456	-.0455	-.0455	-.0451	-.0441	-.0426	-.0408	-.0388	-.0366	-.0345	-.0324	-.0303

Values of w/w_0 for z^* of -

TABLE III.
CALCULATED VALUES OF INDUCED-VELOCITY RATIO, w/w_0 , IN THE LATERAL PLANE
OF A ROTOR WITH UNIT SINE VORTICITY, $\chi = \tan^{-1} 4 = 75.97^\circ$.

y^*	Values of w/w_0 for z^* of -															
	0	0.05	0.1	0.15	0.2	0.25	0.3	0.4	0.5	0.6	0.7	0.8	0.85	0.9	0.95	1.00
0	0	0	0	0	0	0	0	0	0	0	0	0	0	0	0	0
.1	.2747	.2913	.3486	.2587	.2009	.1609	.1514	.0908	.0642	.0458	.0327	.0234	.0196	.0166	.0139	.0116
.2	.589	.4203	.4029	.4213	.3470	.2879	.2404	.1699	.1214	.0870	.0622	.0443	.0374	.0314	.0263	.0220
.3	.932	.5355	.4866	.6597	.3407	.3752	.3190	.2305	.1661	.1195	.0857	.0611	.0511	.0432	.0361	.0301
.4	.6955	.6305	.5746	.5192	.4984	.4297	.3689	.2696	.1955	.1409	.1010	.0719	.0604	.0506	.0425	.0352
.5	.7780	.7029	.6197	.5571	.5286	.4564	.3921	.2865	.2075	.1493	.1068	.0758	.0636	.0531	.0441	.0365
.6	.8482	.7560	.6599	.5907	.5317	.4548	.3876	.2799	.2011	.1440	.1026	.0723	.0604	.0502	.0415	.0340
.7	.9216	.7932	.6769	.5772	.4986	.4177	.3502	.2475	.1935	.1251	.0855	.0619	.0513	.0423	.0344	.0278
.8	.9788	.7930	.6281	.5109	.4087	.3513	.2720	.1883	.1330	.0943	.0662	.0452	.0372	.0300	.0258	.0183
.85	1.0054	.7546	.5602	.4283	.3320	.2649	.2159	.1435	.1060	.0752	.0526	.0355	.0268	.0225	.0173	.0127
.9	1.0350	.6648	.5336	.3037	.2910	.1825	.1499	.1062	.0766	.0547	.0378	.0248	.0193	.0115	.0102	.0065
.95	1.0600	.4015	.1966	.1315	.1041	.0886	.0777	.0604	.0459	.0333	.0225	.0134	.0095	.0060	.0028	.0001
1.0	-	.2800	-.1340	-.0659	-.0289	-.0076	.0046	.0116	.0151	.0117	.0065	.0018	-.0006	-.0027	-.0048	-.0067
1.05	-1.5380	-.7640	-.3987	-.2334	-.1456	-.0942	-.0622	-.0284	-.0144	-.0094	-.0038	-.0025	-.0116	-.0125	-.0135	
1.1	-1.0631	-.7591	-.4999	-.3331	-.2289	-.1620	-.1077	-.0666	-.0416	-.0293	-.0210	-.0204	-.0202	-.0203	-.0203	
1.15	-.8191	-.6663	-.5044	-.3731	-.2770	-.2084	-.1594	-.0986	-.0657	-.0476	-.0374	-.0318	-.0287	-.0277	-.0277	
1.2	-.6683	-.5788	-.4747	-.3782	-.2984	-.2359	-.1880	-.1237	-.0861	-.0657	-.0501	-.0419	-.0350	-.0367	-.0375	
1.3	-.4905	-.4008	-.3388	-.2765	-.2176	-.1553	-.1161	-.0895	-.0717	-.0596	-.0476	-.0375	-.0350	-.0350	-.0350	
1.4	-.3886	-.2761	-.2554	-.2218	-.1979	-.1692	-.1355	-.1069	-.0876	-.0775	-.0680	-.0632	-.0592	-.0556	-.0556	
1.6	-.2134	-.2045	-.1899	-.1620	-.1516	-.1106	-.1037	-.1226	-.1052	-.0910	-.0850	-.0797	-.0749	-.0706	-.0706	
2.0	-.1774	-.1708	-.1219	-.1185	-.1114	-.1099	-.1050	-.0999	-.0749	-.0626	-.0526	-.0442	-.0401	-.0331	-.0331	
2.5	-.1246	-.0969	-.0955	-.0798	-.0778	-.0717	-.0693	-.0688	-.0641	-.0513	-.0413	-.0349	-.0273	-.0225	-.0201	
3.0	-.0778	-.0660	-.0674	-.0667	-.0590	-.0584	-.0766	-.0732	-.0737	-.0720	-.0704	-.0686	-.0676	-.0658	-.0648	
3.5	-.0593	-.0327	-.0324	-.0472	-.0475	-.0432	-.0516	-.0511	-.0506	-.0501	-.0474	-.0485	-.0482	-.0478	-.0475	
4.0	-.0432	-.0430	-.0428	-.0430	-.0426	-.0423	-.0426	-.0420	-.0416	-.0412	-.0409	-.0406	-.0405	-.0403	-.0401	

TABLE III.
CONTINUED.

y^*	Values of w/w_0 for $z \neq 0$																
	1.05	1.1	1.15	1.2	1.3	1.4	1.6	1.8	2.0	2.5	3.0	3.5	4.0	4.5	5.0	5.5	6.0
0	0	.0036	.0080	.0065	.0074	0	.0020	0	.0014	0	0	0	.0010	-.0008	0	0	0
.1	.0	.0151	.0123	.0100	.0064	.0038	.0003	.0015	.0024	.0027	-.0019	-.0013	-.0016	-.0016	-.0005	0	0
.2	.0182	.0250	.0206	.0168	.0136	.0085	.0047	0	.0025	.0037	-.0044	-.0040	-.0034	-.0028	-.0020	-.0012	-.0010
.3	.0290	.0238	.0193	.0155	.0094	.0049	.0019	.0008	.0037	.0052	-.0060	-.0055	-.0045	-.0038	-.0032	-.0017	-.0017
.4	.0243	.0195	.0154	.0088	.0039	.0021	.0005	.0068	.0075	.0067	-.0057	-.0047	-.0032	-.0027	-.0023	-.0020	-.0020
.5	.0299	.0243	.0195	.0154	.0088	.0039	.0021	.0005	.0068	.0075	-.0067	-.0057	-.0047	-.0033	-.0028	-.0024	-.0024
.6	.0276	.0220	.0173	.0132	.0067	.0019	.0041	-.0012	.0087	.0092	-.0081	-.0068	-.0057	-.0048	-.0040	-.0034	-.0030
.7	.0220	.0170	.0127	.0091	.0032	.0012	.0067	-.0095	.0107	.0107	-.0093	-.0079	-.0066	-.0056	-.0047	-.0039	-.0035
.8	.0137	.0096	.0061	.0031	.0017	.0004	.0053	-.0099	.0121	.0130	-.0124	-.0108	-.0090	-.0075	-.0063	-.0054	-.0045
.85	.0087	.0052	.0022	.0004	.0047	.0004	.0077	-.0116	.0116	.0135	-.0141	-.0133	-.0114	-.0096	-.0080	-.0071	-.0057
.9	.0033	.0004	.0020	.0042	.0078	.0104	.0136	-.0150	.0154	.0142	-.0121	-.0101	-.0084	-.0071	-.0059	-.0048	-.0042
.95	-.0024	-.0046	-.0066	-.0083	-.0110	-.0131	-.0155	-.0165	-.0150	-.0127	-.0106	-.0089	-.0071	-.0051	-.0043	-.0034	-.0024
1.0	-.0083	-.0100	-.0113	-.0125	-.0144	-.0159	-.0176	-.0179	-.0159	-.0134	-.0112	-.0094	-.0078	-.0066	-.0057	-.0046	-.0037
1.05	-.0145	-.0123	-.0161	-.0168	-.0179	-.0188	-.0197	-.0197	-.0191	-.0168	-.0141	-.0117	-.0097	-.0082	-.0069	-.0059	-.0051
1.1	-.0204	-.0207	-.0209	-.0216	-.0217	-.0218	-.0213	-.0205	-.0205	-.0176	-.0148	-.0117	-.0097	-.0082	-.0069	-.0059	-.0051
1.15	-.0262	-.0261	-.0258	-.0273	-.0252	-.0240	-.0240	-.0240	-.0240	-.0218	-.0186	-.0154	-.0123	-.0102	-.0085	-.0062	-.0054
1.2	-.0323	-.0313	-.0304	-.0298	-.0287	-.0277	-.0262	-.0262	-.0262	-.0247	-.0217	-.0186	-.0154	-.0128	-.0106	-.0085	-.0065
1.3	-.0411	-.0394	-.0380	-.0355	-.0336	-.0304	-.0290	-.0290	-.0290	-.0288	-.0259	-.0212	-.0161	-.0134	-.0110	-.0093	-.0075
1.4	-.0525	-.0498	-.0454	-.0438	-.0417	-.0390	-.0355	-.0311	-.0294	-.0289	-.0259	-.0212	-.0174	-.0143	-.0120	-.0100	-.0081
1.6	-.0668	-.0632	-.0632	-.0633	-.0592	-.0522	-.0483	-.0483	-.0483	-.0371	-.0322	-.0262	-.0211	-.0173	-.0144	-.0121	-.0102
1.8	-.0751	-.0715	-.0632	-.0632	-.0592	-.0522	-.0477	-.0477	-.0477	-.0420	-.0374	-.0291	-.0233	-.0191	-.0158	-.0133	-.0113
2.0	-.0790	-.0757	-.0726	-.0697	-.0644	-.0598	-.0520	-.0498	-.0498	-.0458	-.0403	-.0316	-.0254	-.0208	-.0173	-.0146	-.0124
2.5	-.0778	-.0756	-.0754	-.0754	-.0712	-.0673	-.0655	-.0655	-.0655	-.0610	-.0460	-.0364	-.0295	-.0245	-.0203	-.0172	-.0148
3.0	-.0711	-.0696	-.0691	-.0691	-.0640	-.0614	-.0563	-.0563	-.0563	-.0516	-.0474	-.0474	-.0466	-.0466	-.0426	-.0392	-.0352
3.5	-.0639	-.0629	-.0619	-.0619	-.0590	-.0572	-.0534	-.0534	-.0534	-.0499	-.0472	-.0472	-.0466	-.0466	-.0426	-.0392	-.0352
4.0	-.0574	-.0567	-.0560	-.0560	-.0540	-.0527	-.0499	-.0499	-.0499	-.0472	-.0446	-.0446	-.0486	-.0486	-.0426	-.0392	-.0352
4.5	-.0519	-.0513	-.0509	-.0509	-.0501	-.0494	-.0484	-.0484	-.0484	-.0463	-.0443	-.0443	-.0374	-.0374	-.0320	-.0289	-.0289
5.0	-.0472	-.0468	-.0465	-.0465	-.0461	-.0453	-.0445	-.0445	-.0445	-.0430	-.0414	-.0414	-.0350	-.0350	-.0290	-.0226	-.0226
5.5	-.0432	-.0429	-.0426	-.0426	-.0418	-.0412	-.0400	-.0400	-.0400	-.0387	-.0374	-.0374	-.0358	-.0358	-.0321	-.0287	-.0287
6.0	-.0398	-.0396	-.0394	-.0394	-.0387	-.0383	-.0383	-.0383	-.0383	-.0362	-.0352	-.0352	-.0343	-.0343	-.0299	-.0274	-.0274

TABLE III.
CONTINUED.

TABLE III.
CONCLUDED.

γ^*	Values of π/π_0 for z^* of -																	
	-1.05	-1.1	-1.15	-1.2	-1.3	-1.4	-1.6	-1.8	-2.0	-2.5	-3.0	-3.5	-4.0	-4.5	-5.0	-5.5	-6.0	
0	0	.0158	-.0130	.0107	.0087	.0056	.0032	.0004	0	0	0	0	0	0	0	0	0	
.1		.0293	-.0242	.0198	.0162	.0102	.0059	.0004	-.0011	-.0021	-.0021	-.0019	-.0016	-.0011	-.0009	-.0003	0	
.2		.0431	-.0320	.0261	.0211	.0130	.0072	-.0004	-.0025	-.0043	-.0062	-.0073	-.0066	-.0044	-.0026	-.0018	-.0016	
.3		.0412	-.0331	.0253	.0203	.0168	.0095	-.0021	-.0065	-.0065	-.0073	-.0073	-.0065	-.0045	-.0039	-.0029	-.0025	
.4		.0350	-.0257	.0194	.0140	.0054	.0010	-.0027	-.0030	-.0030	-.0031	-.0038	-.0038	-.0036	-.0032	-.0033	-.0033	
.5		.0192	-.0134	.0084	.0042	.0019	.0009	-.0078	-.0142	-.0174	-.0149	-.0151	-.0151	-.0132	-.0111	-.0078	-.0048	
.6		.0010	-.0026	.0026	.0057	.0085	.0129	.0163	.0210	.0238	.0222	.0225	.0208	.0176	.0122	.0066	-.0056	
.7		.85	-.0091	-.0115	-.0157	-.0156	-.0187	-.0210	-.0210	-.0218	-.0217	-.0226	-.0187	-.0156	-.0122	-.0087	-.0074	
.8		.9	-.0198	-.0209	-.0220	-.0220	-.0247	-.0260	-.0260	-.0273	-.0275	-.0269	-.0269	-.0199	-.0150	-.0091	-.0078	
.9		.95	-.0364	-.0366	-.0366	-.0366	-.0362	-.0363	-.0310	-.0309	-.0302	-.0291	-.0291	-.0209	-.0174	-.0098	-.0068	
1.0		1.0	-.0412	-.0400	-.0390	-.0383	-.0372	-.0362	-.0346	-.0330	-.0312	-.0265	-.0221	-.0183	-.0127	-.0088	-.0076	
1.05		1.1	1.15	1.2	1.3	1.4	1.5	1.6	1.7	1.8	1.9	2.0	2.1	2.2	2.3	2.4	2.5	
		1.15	1.2	1.3	1.4	1.5	1.6	1.7	1.8	1.9	2.0	2.1	2.2	2.3	2.4	2.5	2.6	
		1.2	1.3	1.4	1.5	1.6	1.7	1.8	1.9	2.0	2.1	2.2	2.3	2.4	2.5	2.6	2.7	
		1.3	1.4	1.5	1.6	1.7	1.8	1.9	2.0	2.1	2.2	2.3	2.4	2.5	2.6	2.7	2.8	
		1.4	1.5	1.6	1.7	1.8	1.9	2.0	2.1	2.2	2.3	2.4	2.5	2.6	2.7	2.8	2.9	
		1.5	1.6	1.7	1.8	1.9	2.0	2.1	2.2	2.3	2.4	2.5	2.6	2.7	2.8	2.9	3.0	
		1.6	1.7	1.8	1.9	2.0	2.1	2.2	2.3	2.4	2.5	2.6	2.7	2.8	2.9	3.0	3.1	
		1.7	1.8	1.9	2.0	2.1	2.2	2.3	2.4	2.5	2.6	2.7	2.8	2.9	3.0	3.1	3.2	
		1.8	1.9	2.0	2.1	2.2	2.3	2.4	2.5	2.6	2.7	2.8	2.9	3.0	3.1	3.2	3.3	
		1.9	2.0	2.1	2.2	2.3	2.4	2.5	2.6	2.7	2.8	2.9	3.0	3.1	3.2	3.3	3.4	
		2.0	2.1	2.2	2.3	2.4	2.5	2.6	2.7	2.8	2.9	3.0	3.1	3.2	3.3	3.4	3.5	
		2.1	2.2	2.3	2.4	2.5	2.6	2.7	2.8	2.9	3.0	3.1	3.2	3.3	3.4	3.5	3.6	
		2.2	2.3	2.4	2.5	2.6	2.7	2.8	2.9	3.0	3.1	3.2	3.3	3.4	3.5	3.6	3.7	
		2.3	2.4	2.5	2.6	2.7	2.8	2.9	3.0	3.1	3.2	3.3	3.4	3.5	3.6	3.7	3.8	
		2.4	2.5	2.6	2.7	2.8	2.9	3.0	3.1	3.2	3.3	3.4	3.5	3.6	3.7	3.8	3.9	
		2.5	2.6	2.7	2.8	2.9	3.0	3.1	3.2	3.3	3.4	3.5	3.6	3.7	3.8	3.9	4.0	
		2.6	2.7	2.8	2.9	3.0	3.1	3.2	3.3	3.4	3.5	3.6	3.7	3.8	3.9	4.0	4.1	
		2.7	2.8	2.9	3.0	3.1	3.2	3.3	3.4	3.5	3.6	3.7	3.8	3.9	4.0	4.1	4.2	
		2.8	2.9	3.0	3.1	3.2	3.3	3.4	3.5	3.6	3.7	3.8	3.9	4.0	4.1	4.2	4.3	
		2.9	3.0	3.1	3.2	3.3	3.4	3.5	3.6	3.7	3.8	3.9	4.0	4.1	4.2	4.3	4.4	
		3.0	3.1	3.2	3.3	3.4	3.5	3.6	3.7	3.8	3.9	4.0	4.1	4.2	4.3	4.4	4.5	
		3.1	3.2	3.3	3.4	3.5	3.6	3.7	3.8	3.9	4.0	4.1	4.2	4.3	4.4	4.5	4.6	
		3.2	3.3	3.4	3.5	3.6	3.7	3.8	3.9	4.0	4.1	4.2	4.3	4.4	4.5	4.6	4.7	
		3.3	3.4	3.5	3.6	3.7	3.8	3.9	4.0	4.1	4.2	4.3	4.4	4.5	4.6	4.7	4.8	
		3.4	3.5	3.6	3.7	3.8	3.9	4.0	4.1	4.2	4.3	4.4	4.5	4.6	4.7	4.8	4.9	
		3.5	3.6	3.7	3.8	3.9	4.0	4.1	4.2	4.3	4.4	4.5	4.6	4.7	4.8	4.9	5.0	
		3.6	3.7	3.8	3.9	4.0	4.1	4.2	4.3	4.4	4.5	4.6	4.7	4.8	4.9	5.0	5.1	
		3.7	3.8	3.9	4.0	4.1	4.2	4.3	4.4	4.5	4.6	4.7	4.8	4.9	5.0	5.1	5.2	
		3.8	3.9	4.0	4.1	4.2	4.3	4.4	4.5	4.6	4.7	4.8	4.9	5.0	5.1	5.2	5.3	
		3.9	4.0	4.1	4.2	4.3	4.4	4.5	4.6	4.7	4.8	4.9	5.0	5.1	5.2	5.3	5.4	
		4.0	4.1	4.2	4.3	4.4	4.5	4.6	4.7	4.8	4.9	5.0	5.1	5.2	5.3	5.4	5.5	
		4.1	4.2	4.3	4.4	4.5	4.6	4.7	4.8	4.9	5.0	5.1	5.2	5.3	5.4	5.5	5.6	
		4.2	4.3	4.4	4.5	4.6	4.7	4.8	4.9	5.0	5.1	5.2	5.3	5.4	5.5	5.6	5.7	
		4.3	4.4	4.5	4.6	4.7	4.8	4.9	5.0	5.1	5.2	5.3	5.4	5.5	5.6	5.7	5.8	
		4.4	4.5	4.6	4.7	4.8	4.9	5.0	5.1	5.2	5.3	5.4	5.5	5.6	5.7	5.8	5.9	
		4.5	4.6	4.7	4.8	4.9	5.0	5.1	5.2	5.3	5.4	5.5	5.6	5.7	5.8	5.9	6.0	
		4.6	4.7	4.8	4.9	5.0	5.1	5.2	5.3	5.4	5.5	5.6	5.7	5.8	5.9	6.0	6.1	
		4.7	4.8	4.9	5.0	5.1	5.2	5.3	5.4	5.5	5.6	5.7	5.8	5.9	6.0	6.1	6.2	
		4.8	4.9	5.0	5.1	5.2	5.3	5.4	5.5	5.6	5.7	5.8	5.9	6.0	6.1	6.2	6.3	
		4.9	5.0	5.1	5.2	5.3	5.4	5.5	5.6	5.7	5.8	5.9	6.0	6.1	6.2	6.3	6.4	
		5.0	5.1	5.2	5.3	5.4	5.5	5.6	5.7	5.8	5.9	6.0	6.1	6.2	6.3	6.4	6.5	
		5.1	5.2	5.3	5.4	5.5	5.6	5.7	5.8	5.9	6.0	6.1	6.2	6.3	6.4	6.5	6.6	
		5.2	5.3	5.4	5.5	5.6	5.7	5.8	5.9	6.0	6.1	6.2	6.3	6.4	6.5	6.6	6.7	
		5.3	5.4	5.5	5.6	5.7	5.8	5.9	6.0	6.1	6.2	6.3	6.4	6.5	6.6	6.7	6.8	
		5.4	5.5	5.6	5.7	5.8	5.9	6.0	6.1	6.2	6.3	6.4	6.5	6.6	6.7	6.8	6.9	
		5.5	5.6	5.7	5.8	5.9	6.0	6.1	6.2	6.3	6.4	6.5	6.6	6.7	6.8	6.9	7.0	
		5.6	5.7	5.8	5.9	6.0	6.1	6.2	6.3	6.4	6.5	6.6	6.7	6.8	6.9	7.0	7.1	
		5.7	5.8	5.9	6.0	6.1	6.2	6.3	6.4	6.5	6.6	6.7	6.8	6.9	7.0	7.1	7.2	
		5.8	5.9	6.0	6.1	6.2	6.3	6.4	6.5	6.6	6.7	6.8	6.9	7.0	7.1	7.2	7.3	
		5.9	6.0	6.1	6.2	6.3	6.4	6.5	6.6	6.7	6.8	6.9	7.0	7.1	7.2	7.3	7.4	
		6.0	6.1	6.2	6.3	6.4	6.5	6.6	6.7	6.8	6.9	7.0	7.1	7.2	7.3	7.4	7.5	

TABLE IV.
CALCULATED VALUES OF INDUCED-VELOCITY RATIO, w/w_0 , IN THE LATERAL PLANE
OF A ROTOR WITH UNIT SINE VORTICITY, $\chi = \tan^{-1} 10 = 84.29^\circ$.

y*	Values of w/w_0 for z^1 of -										
	0	0.02	0.04	0.06	0.08	0.1	0.2	0.3	0.4	0.5	0.6
0	0	0	0	0	0	0	0	0	0	0	0
.1	.4928	.3919	.4005	.3539	.3342	.3263	.3184	.3105	.3025	.3017	.3069
.2	.6388	.6148	.5601	.5517	.5023	.4723	.3880	.2690	.1911	.1366	.0378
.3	.7605	.7326	.6895	.6617	.6297	.5893	.5643	.5360	.5277	.5186	.5338
.4	.8455	.8144	.7744	.7350	.6944	.6728	.6277	.5089	.2993	.2171	.1565
.5	.9205	.8788	.8374	.7964	.7561	.7265	.5587	.4307	.3147	.2279	.1640
.6	.9802	.9320	.8845	.8577	.7985	.7540	.6634	.4199	.3024	.2170	.1252
.7	1.0348	.9782	.9177	.8585	.8012	.785	.5251	.3690	.2598	.1842	.1307
.8	1.0897	.9974	.9083	.8221	.7413	.6711	.5151	.2707	.1309	.0926	.0644
.85	1.1152	.9886	.8661	.7952	.6562	.5732	.3168	.2011	.1385	.0983	.0442
.9	1.1403	.9365	.7510	.5989	.4802	.3919	.2869	.1204	.0364	.0697	.0321
.95	1.1725	.7050	.3877	.2151	.1233	.0764	.0315	.0335	.0321	.0193	.0144
1.0	1.2146	-.8006	-.5779	-.4402	-.3459	-.1268	-.0516	-.0208	-.0087	-.0050	.0060
1.05	1.2996	-.1303	-.1006	-.7885	-.6307	-.2563	-.1263	-.0693	-.0422	-.0290	-.0207
1.1	1.1245	-.1164	-.1048	-.7972	-.6869	-.3380	-.1849	-.1108	-.0722	-.0513	-.0397
1.15	1.2443	-.8818	-.8342	-.7751	-.6411	-.3754	-.2256	-.1441	-.0880	-.0712	-.0552
1.2	1.1323	-.7137	-.6866	-.6149	-.5743	-.3827	-.2502	-.1688	-.1191	-.0685	-.0641
1.3	1.5233	-.4174	-.3574	-.3270	-.2656	-.2045	-.1629	-.1183	-.1148	-.0216	-.0568
1.4	1.4085	-.2856	-.2126	-.2216	-.2216	-.1930	-.1662	-.1312	-.1077	-.0403	-.0758
1.6	1.2208	-.2144	-.2030	-.1684	-.1720	-.1554	-.1394	-.1230	-.1068	-.0996	-.0336
2.0	1.1809	-.1771	-.1707	-.1621	-.1521	-.1154	-.114	-.11306	-.1200	-.1058	-.1003
2.5	1.260	-.1246	-.1223	-.1123	-.1123	-.1116	-.1112	-.1067	-.1019	-.0370	-.0336
3.0	1.0977	-.0970	-.0958	-.0744	-.0726	-.0705	-.0683	-.0683	-.0677	-.0617	-.0221
3.5	1.0802	-.0797	-.0791	-.0783	-.0774	-.0762	-.0746	-.0734	-.0716	-.0710	-.0776
4.0	1.0683	-.0680	-.0675	-.0671	-.0664	-.0657	-.0649	-.0639	-.0624	-.0701	-.0684
4.5	1.0596	-.0594	-.0591	-.0587	-.0583	-.0578	-.0572	-.0566	-.0559	-.0551	-.0613
5.0	1.0529	-.0528	-.0525	-.0520	-.0516	-.0512	-.0508	-.0503	-.0500	-.0498	-.0548
5.5	1.0476	-.0475	-.0473	-.0469	-.0467	-.0463	-.0460	-.0455	-.0452	-.0450	-.045
6.0	1.0433	-.0432	-.0432	-.0430	-.0428	-.0426	-.0424	-.0421	-.0418	-.0415	-.0411

TABLE IV.
CONTINUED.

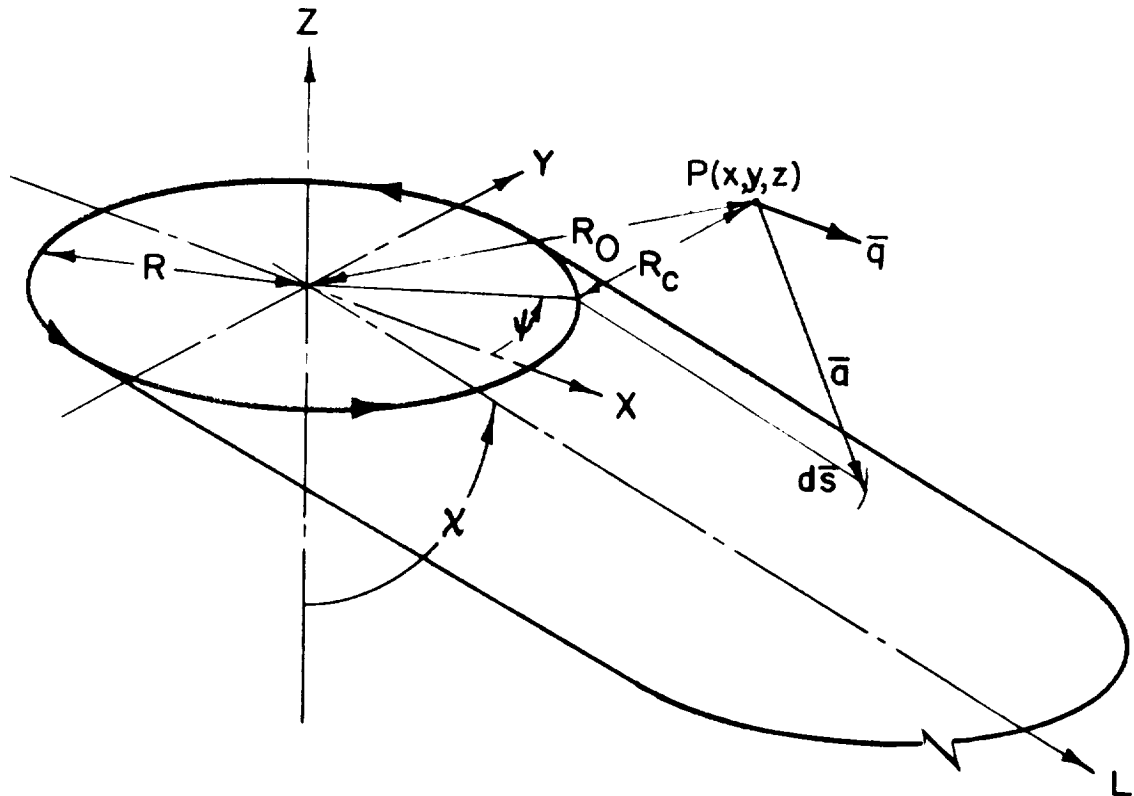
Y ¹	Values of w/w ₀ for z = 0 -											
	1.05	1.1	1.15	1.2	1.3	1.4	1.6	1.8	2.0	2.5	3.0	3.5
0	0	0	0	.0061	0	.0023	0	0	.0016	-.0015	0	0
.1	.0109	.0030	.0074	.0061	0	.0038	.0002	-.0013	-.0015	-.0011	-.0008	0
.2	.0206	.0169	.0139	.0113	.0072	.0042	.0003	-.0027	-.0037	-.0030	-.0026	-.0015
.3	.0277	.0231	.0188	.0152	.0053	.0028	.0001	-.0042	-.0050	-.0045	-.0037	-.0023
.4	.0321	.0264	.0213	.0171	.0103	.0053	.0010	-.0042	-.0058	-.0067	-.0060	-.0023
.5	.0327	.0265	.0213	.0167	.0051	.0026	.0001	-.0061	-.0076	-.0055	-.0075	-.0053
.6	.0293	.0233	.0182	.0138	.0068	.0016	-.0050	-.0083	-.0009	-.0103	-.0031	-.0064
.7	.0223	.0171	.0126	.0087	.0024	-.0027	-.0081	-.0110	-.0123	-.0122	-.0106	-.0054
.8	.0123	.0051	.0046	.0015	.0023	-.0072	-.0118	-.0140	-.0147	-.0141	-.0121	-.0075
.9	.0063	.0029	-.0001	-.0028	-.0069	-.0100	-.0139	-.0156	-.0162	-.0151	-.0129	-.0090
1.0	.0070	-.0002	-.0092	-.0052	-.0173	-.0150	-.0151	-.0171	-.0176	-.0161	-.0136	-.0095
1.1	.0159	-.0150	-.0160	-.0169	-.0185	-.0136	-.0163	-.0132	-.0132	-.0171	-.0145	-.0067
1.2	.0209	-.0213	-.0216	-.0220	-.0225	-.0229	-.0232	-.0228	-.0220	-.0191	-.0159	-.0067
1.3	.0276	-.0275	-.0272	-.0270	-.0266	-.0261	-.0257	-.0255	-.0235	-.0201	-.0167	-.0067
1.4	.0347	-.0346	-.0327	-.0320	-.0306	-.0298	-.0296	-.0282	-.0266	-.0220	-.0174	-.0060
1.5	.0412	-.0395	-.0390	-.0368	-.0348	-.0351	-.0306	-.0285	-.0265	-.0221	-.0182	-.0073
1.6	.0532	-.0504	-.0498	-.0479	-.0429	-.0398	-.0355	-.0322	-.0295	-.0240	-.0197	-.0075
1.7	.0674	-.0592	-.0568	-.0541	-.0425	-.0458	-.0401	-.0358	-.0259	-.0210	-.0162	-.0082
1.8	.0782	-.0740	-.0705	-.0668	-.0691	-.0660	-.0682	-.0582	-.0424	-.0378	-.0236	-.0071
1.9	.0860	-.0820	-.0782	-.0747	-.0685	-.0631	-.0694	-.0677	-.0477	-.0323	-.0195	-.0096
2.0	.0880	-.0853	-.0819	-.0787	-.0728	-.0675	-.0587	-.0417	-.0460	-.0356	-.0285	-.0085
2.1	.0850	-.0827	-.0804	-.0782	-.0741	-.0701	-.0629	-.0566	-.0511	-.0405	-.0228	-.0075
2.2	.0762	-.0747	-.0733	-.0720	-.0642	-.0665	-.0612	-.0565	-.0521	-.0427	-.0297	-.0103
2.3	.0676	-.0647	-.0638	-.0630	-.0588	-.0611	-.0575	-.0540	-.0505	-.0420	-.0277	-.0124
2.4	.0602	-.0595	-.0590	-.0583	-.0558	-.0532	-.0532	-.0504	-.0480	-.0419	-.0277	-.0157
2.5	.0440	-.0375	-.0352	-.0327	-.0218	-.0205	-.0190	-.0171	-.0151	-.0133	-.0145	-.0163
2.6	.0489	-.0486	-.0482	-.0480	-.0475	-.0467	-.0452	-.0457	-.0422	-.0358	-.0249	-.0198
2.7	.0443	-.0441	-.0439	-.0434	-.0434	-.0419	-.0419	-.0407	-.0375	-.0364	-.0276	-.0177
2.8	.0447	-.0443	-.0408	-.0407	-.0401	-.0401	-.0397	-.0397	-.0370	-.0370	-.0271	-.0184
2.9	.0419	-.0408	-.0408	-.0407	-.0401	-.0401	-.0397	-.0397	-.0375	-.0375	-.0271	-.0166
3.0	.0410	-.0408	-.0408	-.0407	-.0401	-.0401	-.0397	-.0397	-.0370	-.0370	-.0271	-.0161

TABLE IV.

CONTINUED.

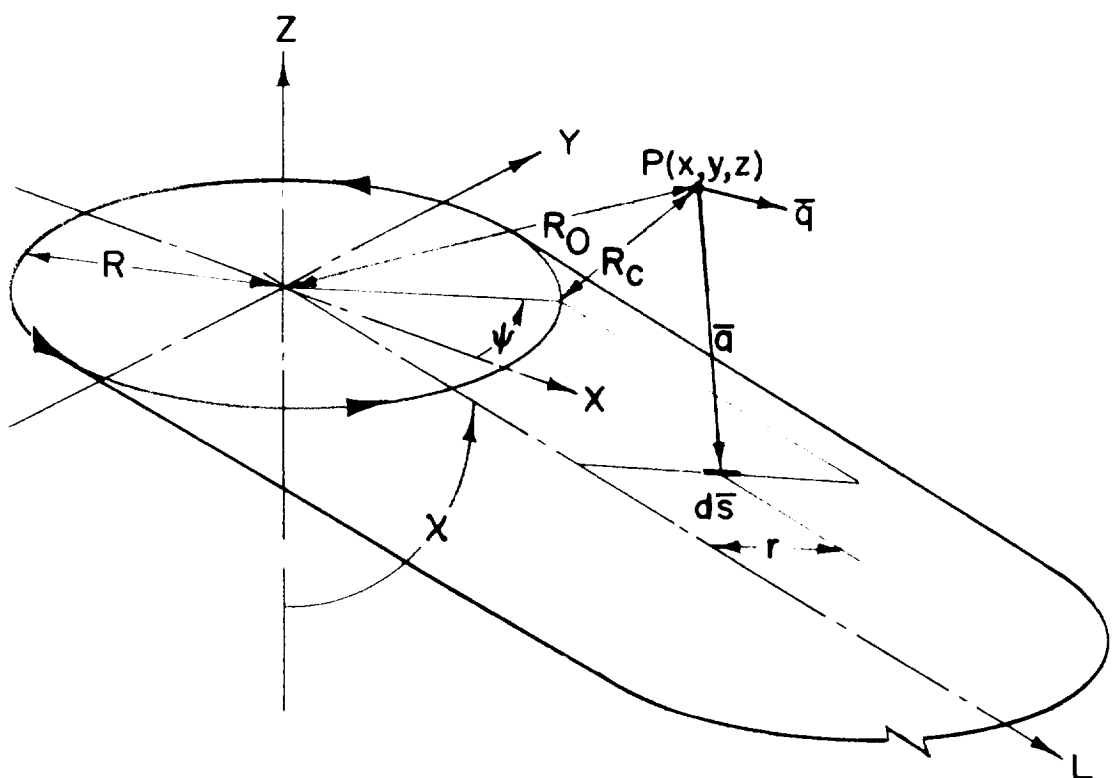
TABLE IV.
CONCLUDED.

γ^*	-1.05	-1.1	-1.15	-1.2	-1.3	-1.4	-1.6	-1.8	-2.0	-2.5	-3.0	-3.5	-4.0	-4.5	-5.0	-5.5	-6.0
Values of w/w_c for $z \approx 1$ at																	
0	0	.0133	.0110	0	0	0	0	0	0	0	0	0	0	0	0	0	0
.1	.0133	.0248	.0205	.0169	.0137	.0087	.0048	.0028	.0003	-.0003	-.0016	-.0012	-.0011	0	0	0	0
.2	.0248	.0354	.0275	.0225	.0181	.0112	.0062	.0030	-.0021	-.0035	-.0051	-.0032	-.0026	-.0022	-.0019	-.0016	-.0006
.3	.0354	.0378	.0307	.0250	.0200	.0113	.0060	.0015	-.0001	-.0015	-.0053	-.0025	-.0049	-.0023	-.0019	-.0014	-.0001
.4	.0378	.0373	.0295	.0240	.0187	.0103	.0036	.0012	-.0002	-.0036	-.0072	-.0032	-.0062	-.0032	-.0023	-.0024	-.0020
.5	.0373	.0318	.0251	.0193	.0144	.0064	.0006	-.0068	-.0106	-.0123	-.0126	-.0111	-.0078	-.0065	-.0017	-.0040	-.0034
.6	.0318	.0217	.0160	.0112	.0070	.0003	-.0003	-.0047	-.0103	-.0110	-.0154	-.0130	-.0103	-.0076	-.0055	-.0017	-.0041
.7	.0217	.0077	.0038	.0003	-.0027	-.0014	-.0014	-.0149	-.0179	-.0176	-.0186	-.0173	-.0150	-.0124	-.0096	-.0025	-.0047
.8	.0077	.0002	-.0033	-.0060	-.0084	-.0122	-.0150	-.0185	-.0200	-.0203	-.0185	-.0159	-.0124	-.0104	-.0087	-.0073	-.0063
.9	.0002	-.0087	-.0108	-.0126	-.0163	-.0170	-.0159	-.0214	-.0222	-.0221	-.0197	-.0167	-.0140	-.0116	-.0092	-.0078	-.0066
.05	-.0174	-.0186	-.0196	-.0204	-.0220	-.0231	-.0231	-.0244	-.0244	-.0231	-.0210	-.0177	-.0147	-.0121	-.0102	-.0086	-.0070
1.0	-.0263	-.0264	-.0265	-.0268	-.0270	-.0274	-.0273	-.0267	-.0257	-.0222	-.0186	-.0154	-.0128	-.0107	-.0090	-.0078	-.0064
1.05	-.0380	-.0362	-.0336	-.0330	-.0330	-.0334	-.0316	-.0304	-.0291	-.0275	-.0254	-.0234	-.0195	-.0156	-.0134	-.0112	-.0081
1.1	-.0457	-.0447	-.0405	-.0393	-.0371	-.0359	-.0351	-.0345	-.0341	-.0294	-.0246	-.0204	-.0169	-.0141	-.0118	-.0100	-.0085
1.15	-.0518	-.0493	-.0438	-.0454	-.0425	-.0401	-.0366	-.0338	-.0313	-.0279	-.0213	-.0176	-.0146	-.0122	-.0104	-.0083	-.0074
1.2	-.0596	-.0564	-.0536	-.0537	-.0473	-.0442	-.0396	-.0361	-.0311	-.0270	-.0221	-.0183	-.0152	-.0128	-.0107	-.0092	-.0076
1.3	-.0733	-.0690	-.0653	-.0753	-.0620	-.0588	-.0520	-.0452	-.0406	-.0367	-.0295	-.0239	-.0197	-.0165	-.0137	-.0116	-.0080
1.4	-.0845	-.0931	-.0939	-.0939	-.0751	-.0712	-.0646	-.0612	-.0507	-.0440	-.0403	-.0317	-.0257	-.0210	-.0174	-.0147	-.0125
1.6	-.1053	-.1005	-.0960	-.0917	-.0842	-.0776	-.0768	-.0704	-.0620	-.0526	-.0465	-.0361	-.0289	-.0236	-.0166	-.0140	-.0120
2.0	-.1058	-.1018	-.0979	-.0942	-.0874	-.0813	-.0813	-.0707	-.0667	-.0561	-.0516	-.0398	-.0318	-.0260	-.0216	-.0182	-.0154
2.5	-.0963	-.0941	-.0918	-.0895	-.0852	-.0811	-.0733	-.0663	-.0602	-.0542	-.0511	-.0424	-.0324	-.0272	-.0231	-.0199	-.0159
3.0	-.0839	-.0826	-.0803	-.0774	-.0748	-.0695	-.0646	-.0605	-.0571	-.0523	-.0492	-.0497	-.0426	-.0351	-.0299	-.0257	-.0195
3.5	-.0730	-.0723	-.0712	-.0707	-.0688	-.0660	-.0630	-.0605	-.0571	-.0534	-.0492	-.0474	-.0423	-.0373	-.0315	-.0275	-.0171
4.0	-.0642	-.0637	-.0632	-.0628	-.0617	-.0617	-.0583	-.0559	-.0521	-.0485	-.0450	-.0424	-.0363	-.0367	-.0310	-.0285	-.0187
4.5	-.0571	-.0567	-.0565	-.0561	-.0554	-.0547	-.0521	-.0485	-.0456	-.0424	-.0388	-.0354	-.0311	-.0280	-.0250	-.0224	-.0200
5.0	-.0513	-.0511	-.0507	-.0501	-.0485	-.0473	-.0453	-.0437	-.0427	-.0400	-.0377	-.0341	-.0313	-.0287	-.0259	-.0237	-.0216
5.5	-.0466	-.0464	-.0462	-.0459	-.0453	-.0457	-.0445	-.0437	-.0423	-.0411	-.0396	-.0376	-.0352	-.0329	-.0305	-.0287	-.0260
6.0	-.0426	-.0426	-.0426	-.0423	-.0421	-.0418	-.0418	-.0411	-.0404	-.0391	-.0375	-.0352	-.0333	-.0313	-.0287	-.0265	-.0245



(a) Outer wake.

Figure 1.- Rotor wake system.



(b) Inner wake.

Figure 1.- Concluded.

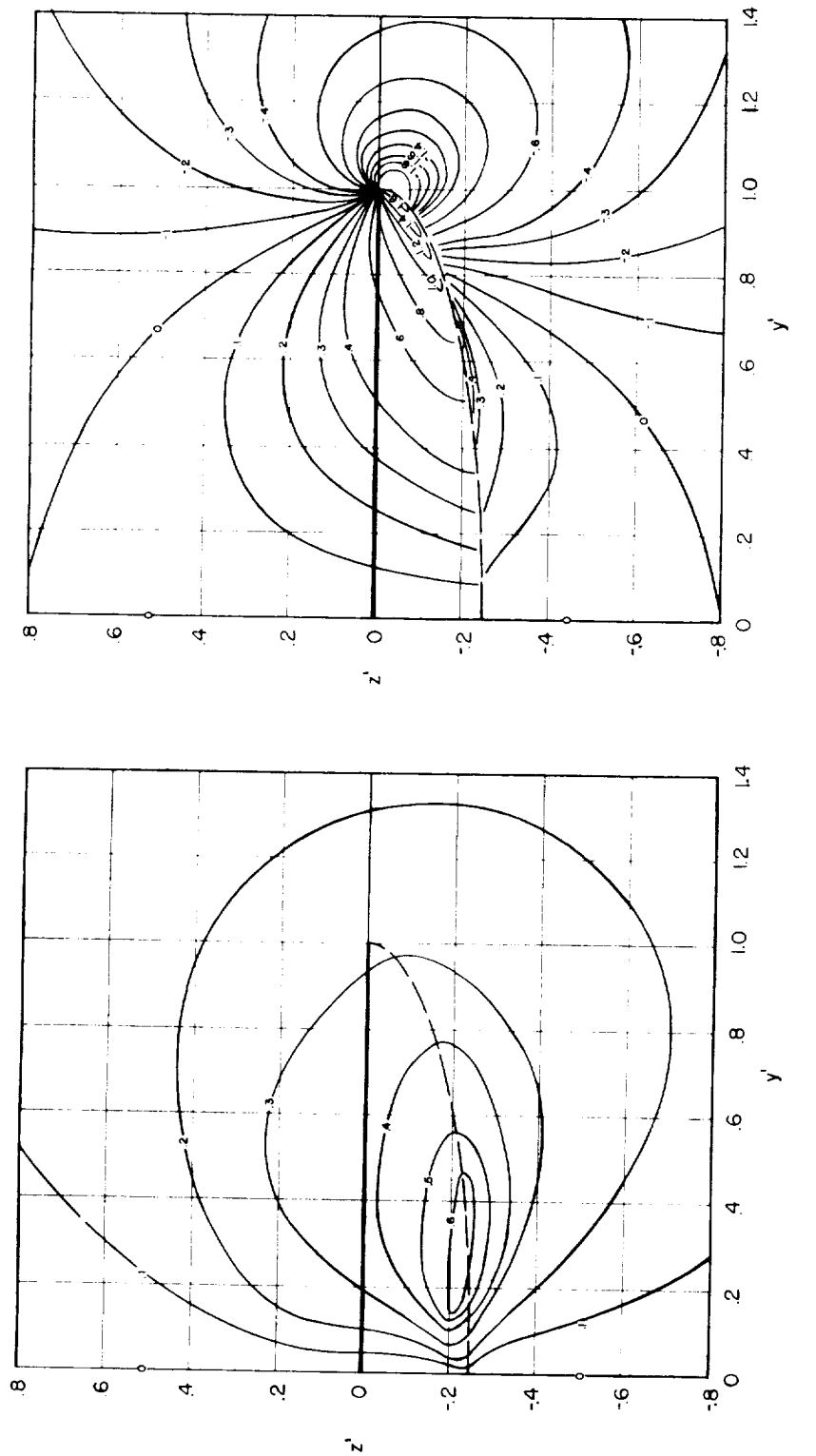


Figure 2.- Contours of induced-velocity ratio, w/w_0 , shown as the individual contributions of the inner and outer wakes in lateral plane of a rotor having a radially uniform unit sin ψ vorticity distribution. Flow fields are antisymmetric about $y' = 0$. Broken line represents edge of wake. $X = \tan^{-1} 4 = 75.97^\circ$.

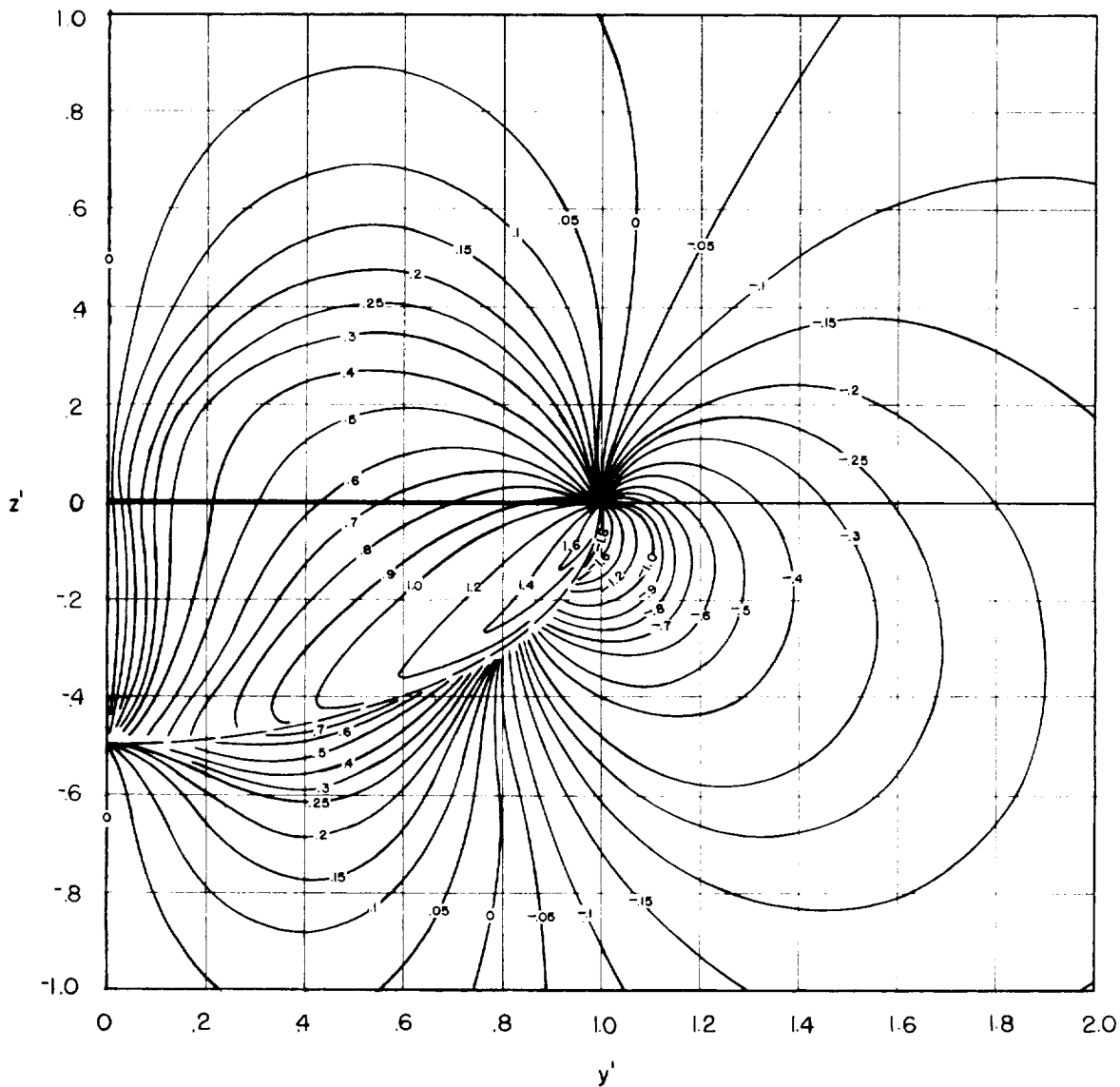
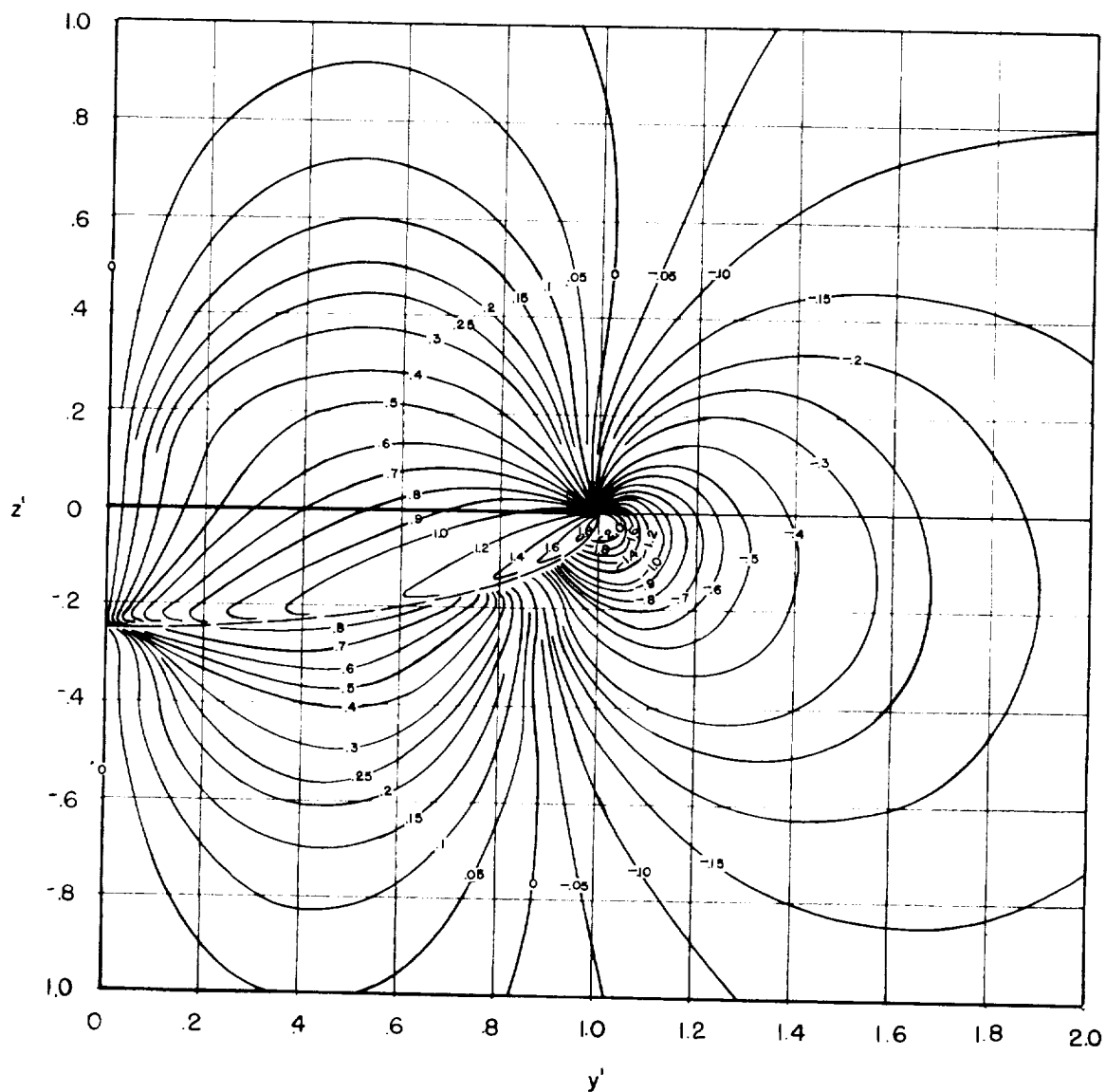
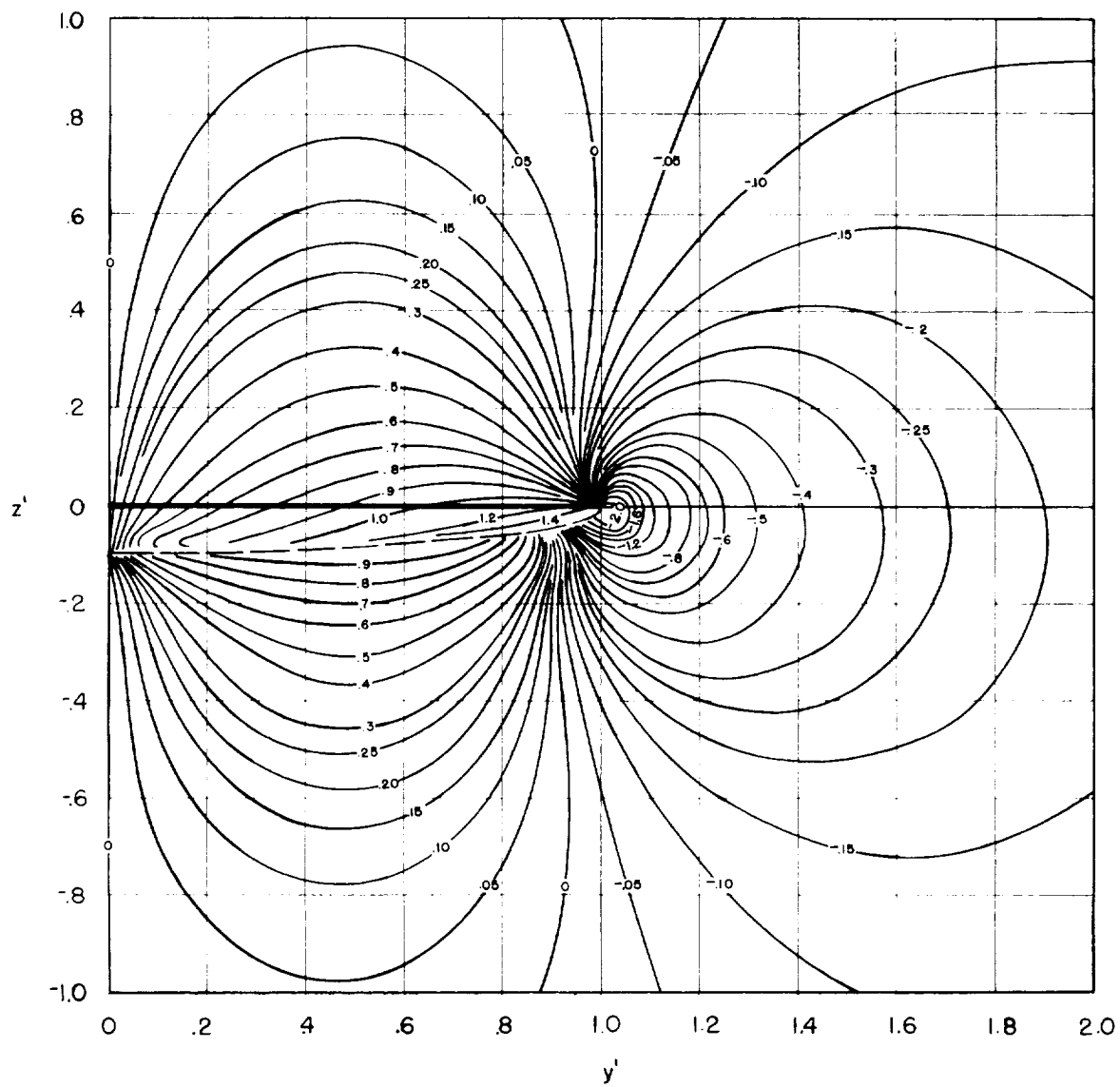


Figure 3.- Contours of induced-velocity ratio, w/w_0 , in the lateral plane in the immediate vicinity of a rotor having a radially uniform unit $\sin \psi$ vorticity distribution. Flow field is antisymmetric about $y' = 0$. Broken line represents edge of wake.



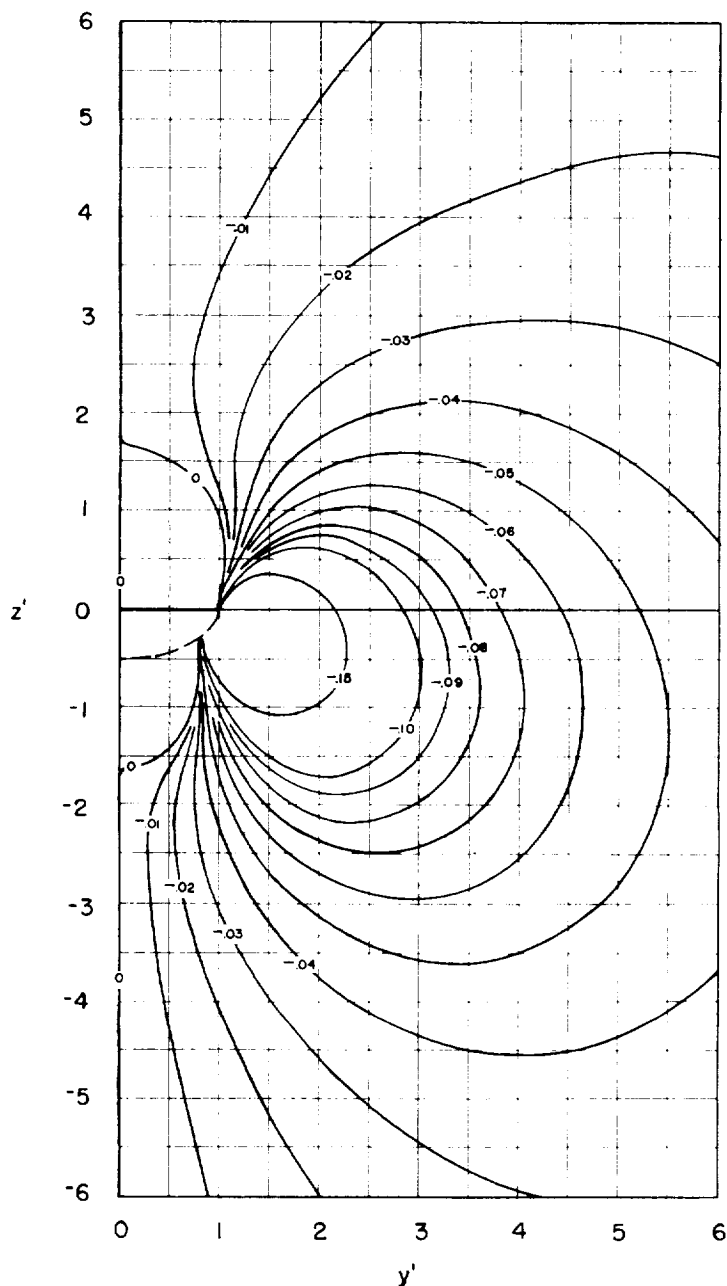
(b) $X = \tan^{-1} 4 = 75.97^\circ$.

Figure 3.- Continued.



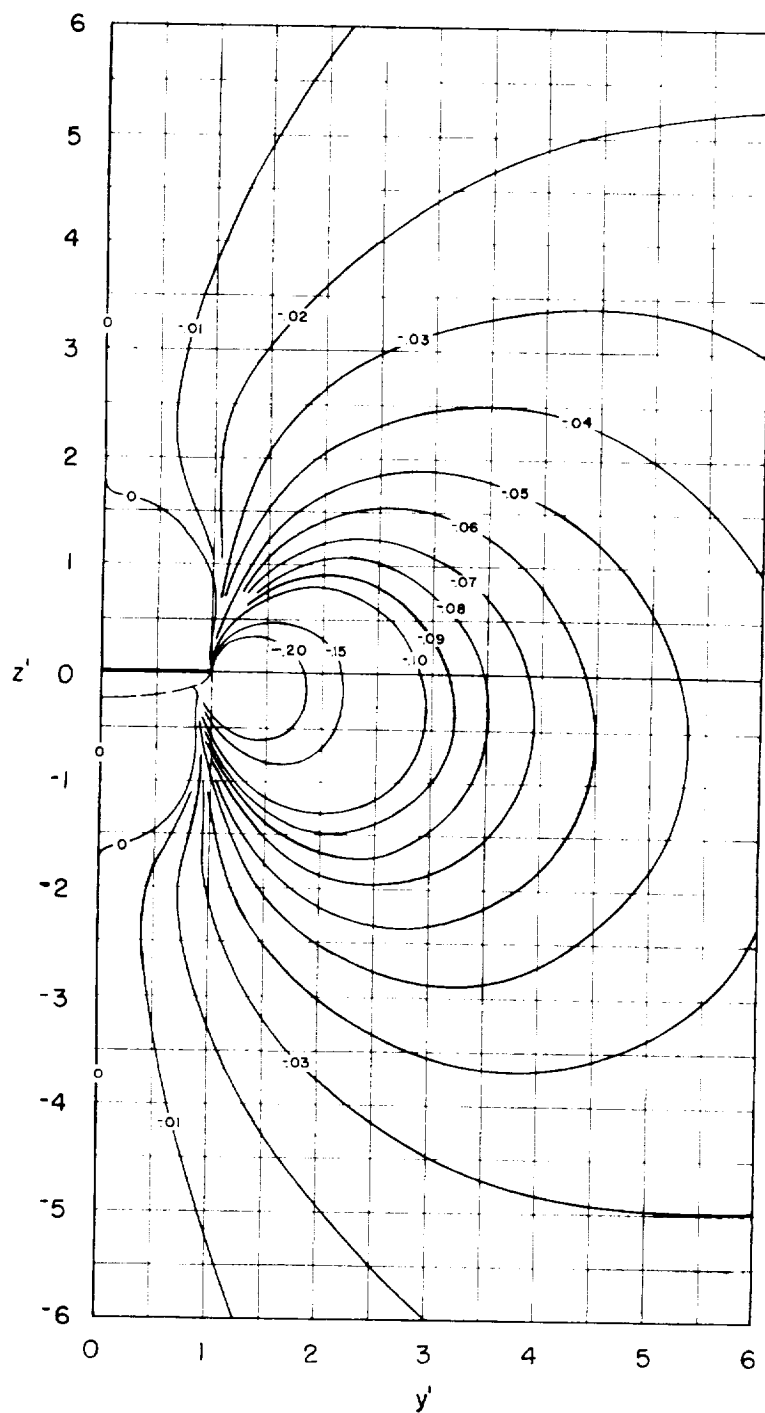
(c) $\chi = \tan^{-1} 10 = 84.29^\circ$.

Figure 3.- Concluded.



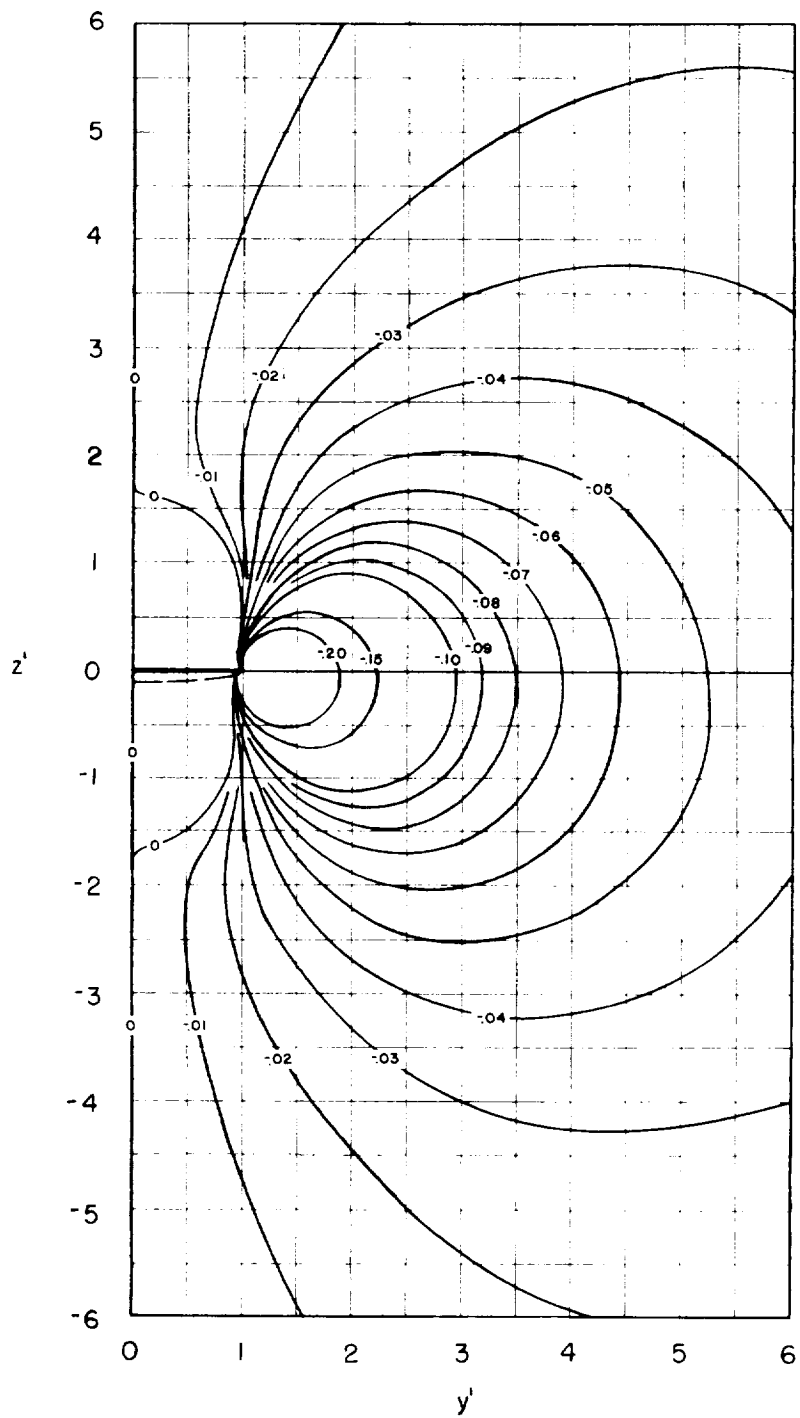
(a) $\chi = \tan^{-1} 2 = 63.43^\circ$.

Figure 4.- Contours of induced-velocity ratio, w/w_0 , outside the wake in the lateral plane of a rotor with a radially uniform unit $\sin \psi$ vorticity distribution. Flow field is antisymmetric about $y' = 0$. Broken line represents edge of wake.



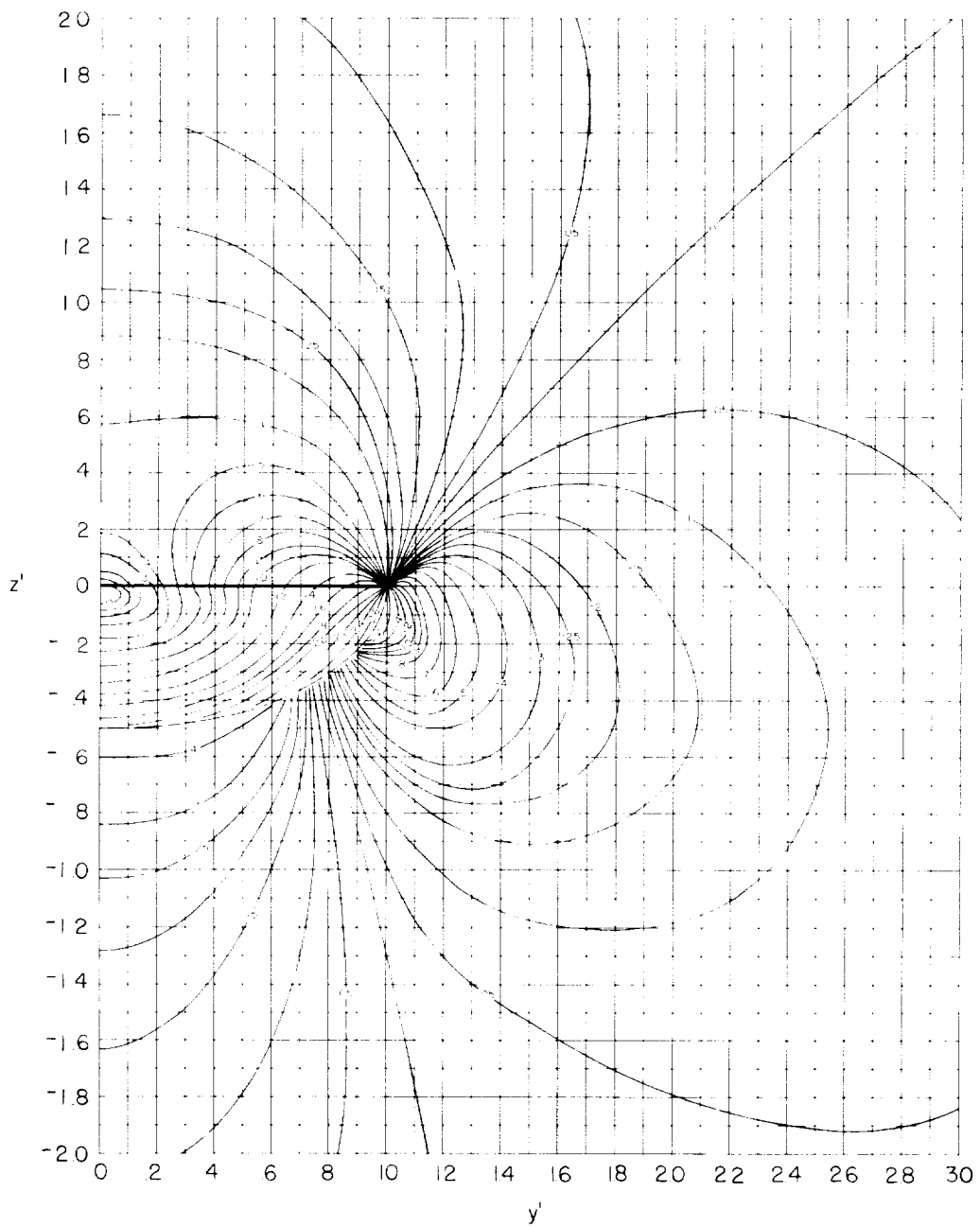
(b) $x = \tan^{-1} 4 = 75.97^\circ$.

Figure 4.- Continued.



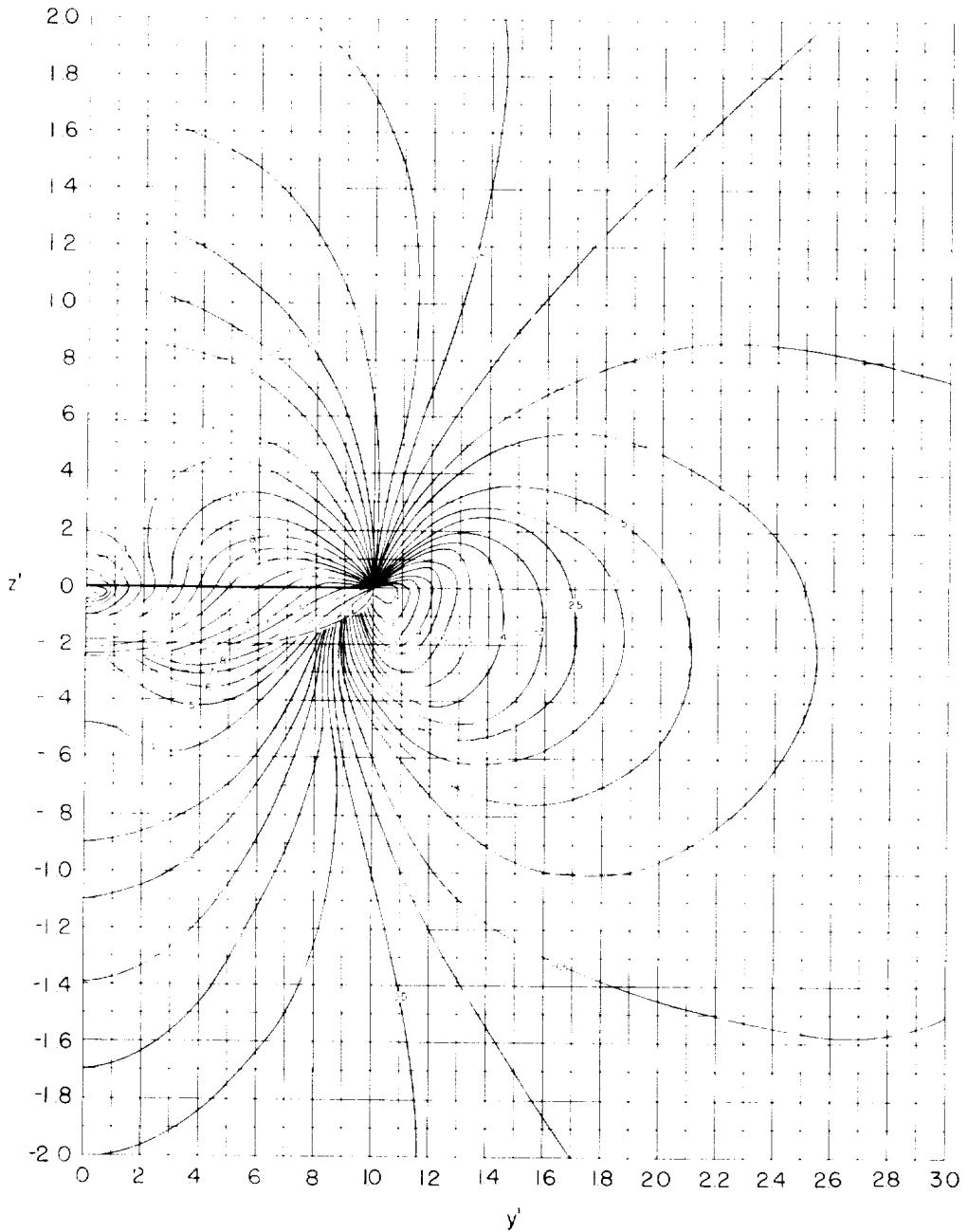
(c) $x = \tan^{-1} 10 = 84.29^\circ$.

Figure 4.- Concluded.



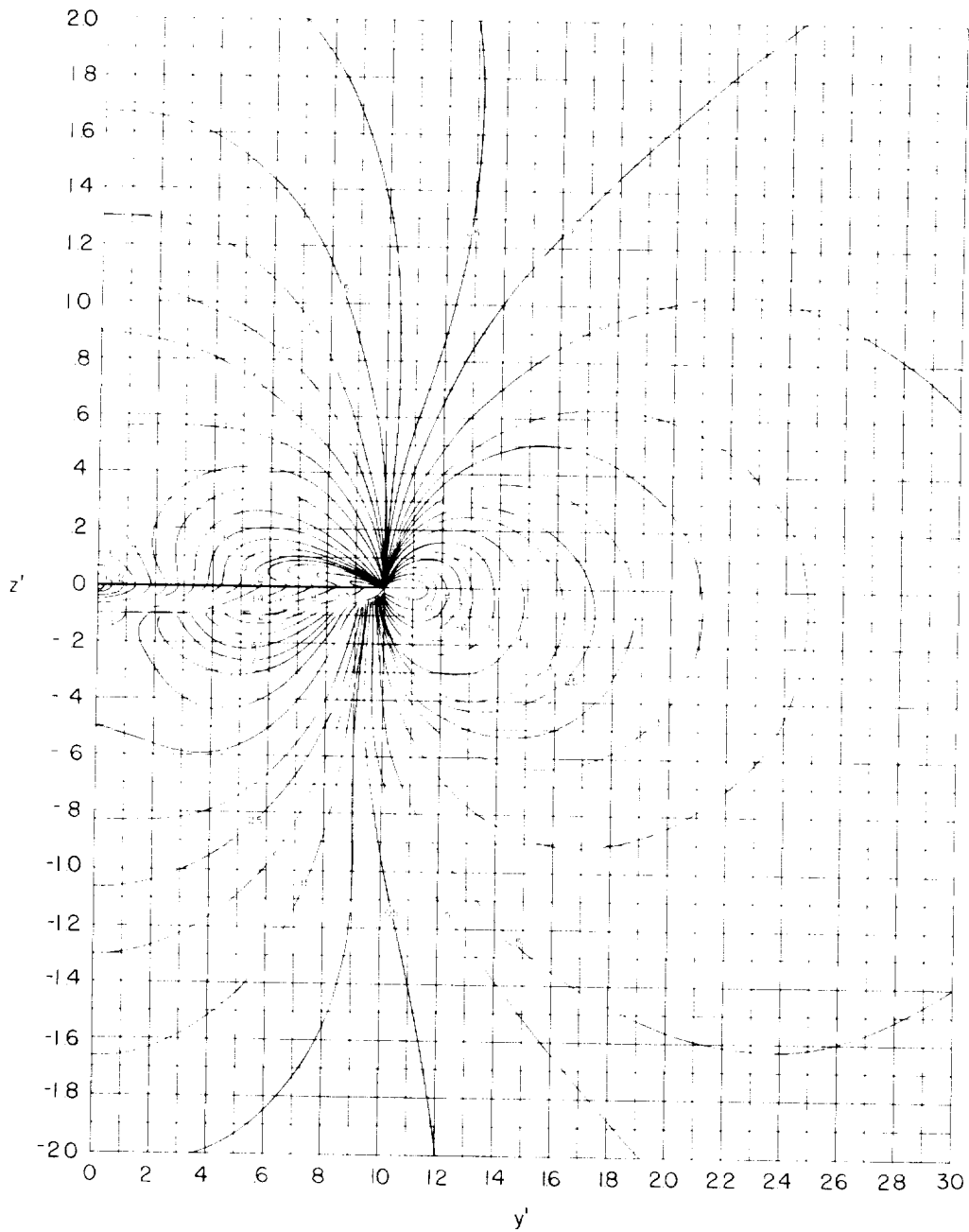
(a) $x = \tan^{-1} 2 = 63.43^\circ$.

Figure 5.- Contours of induced-velocity ratio, w/w_0 , in the lateral plane of a rotor having a triangular, circularly symmetrical vorticity distribution. Flow field is symmetric about $y' = 0$. Broken line represents edge of wake.



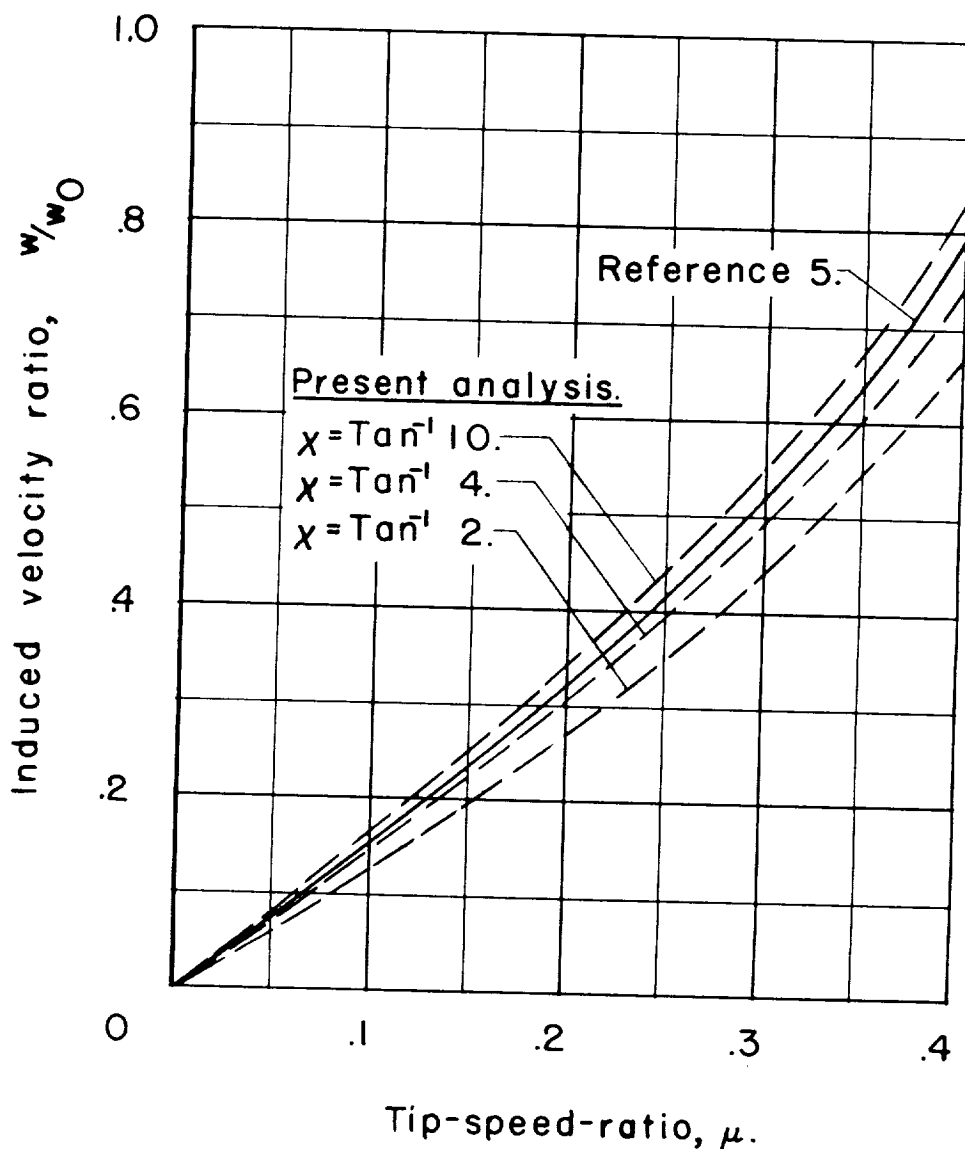
(b) $x = \tan^{-1} 4 = 75.97^\circ$.

Figure 5.- Continued.



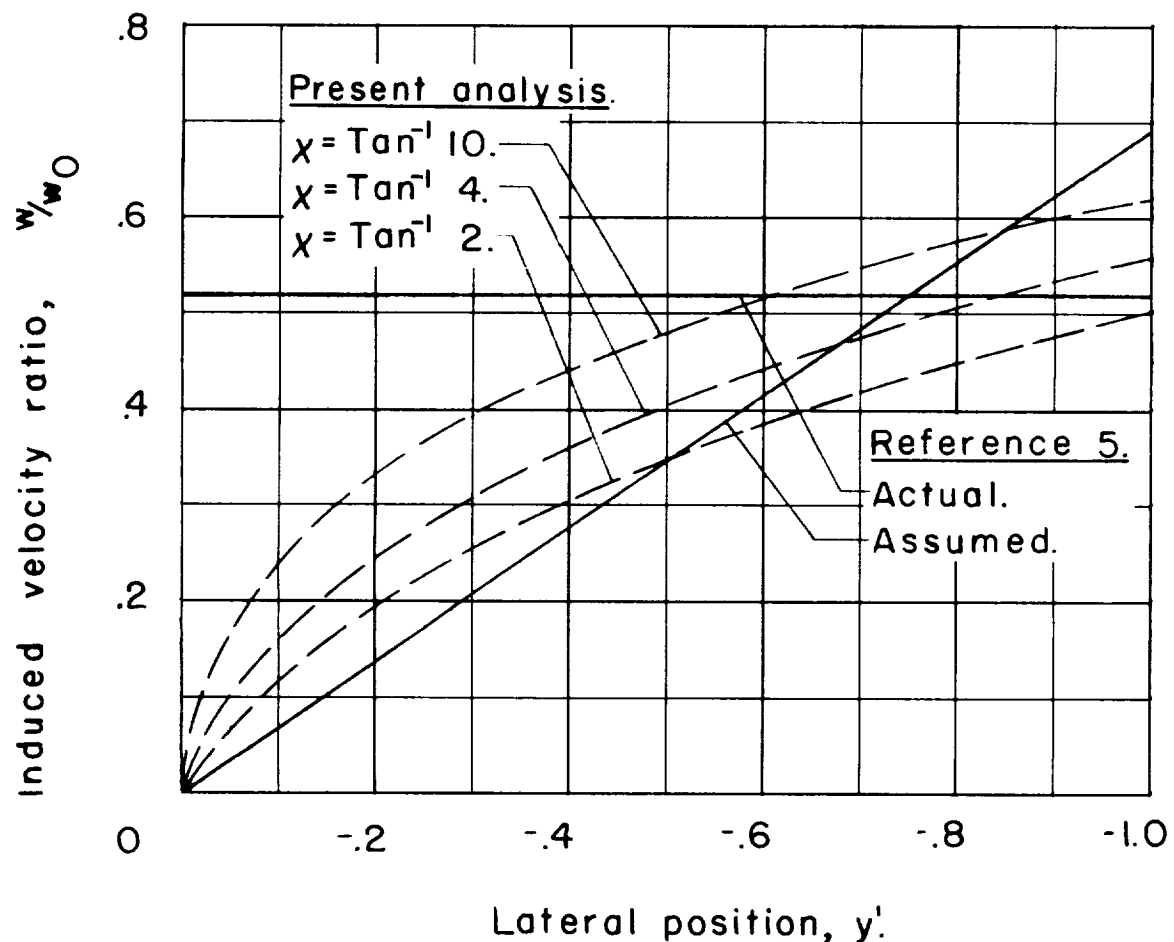
(c) $x = \tan^{-1} 10 = 84.29^\circ$.

Figure 5.- Concluded.



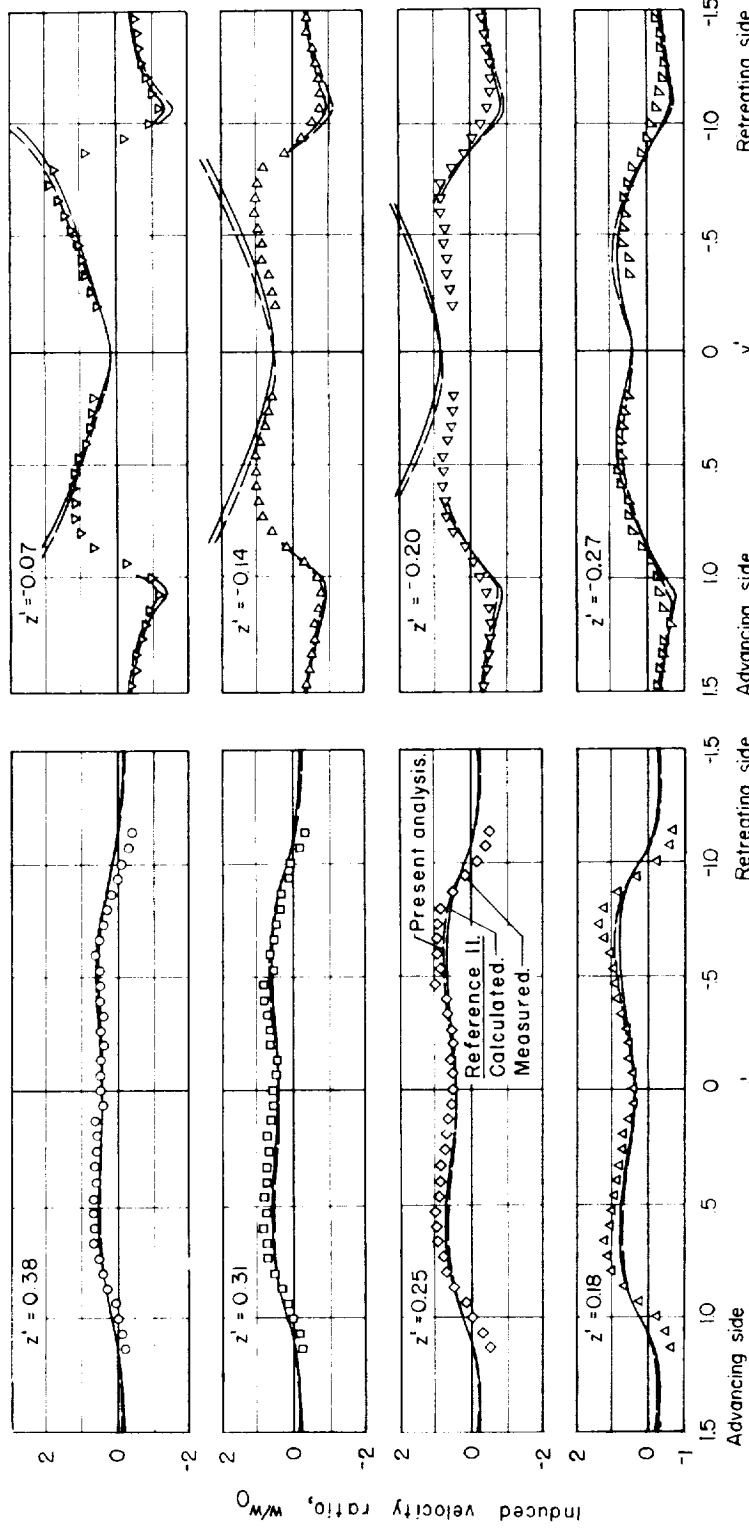
(a) Variation with μ , $y' = -0.75$.

Figure 6.- Comparison, with reference 5, of induced velocities due to asymmetry, lateral axis.



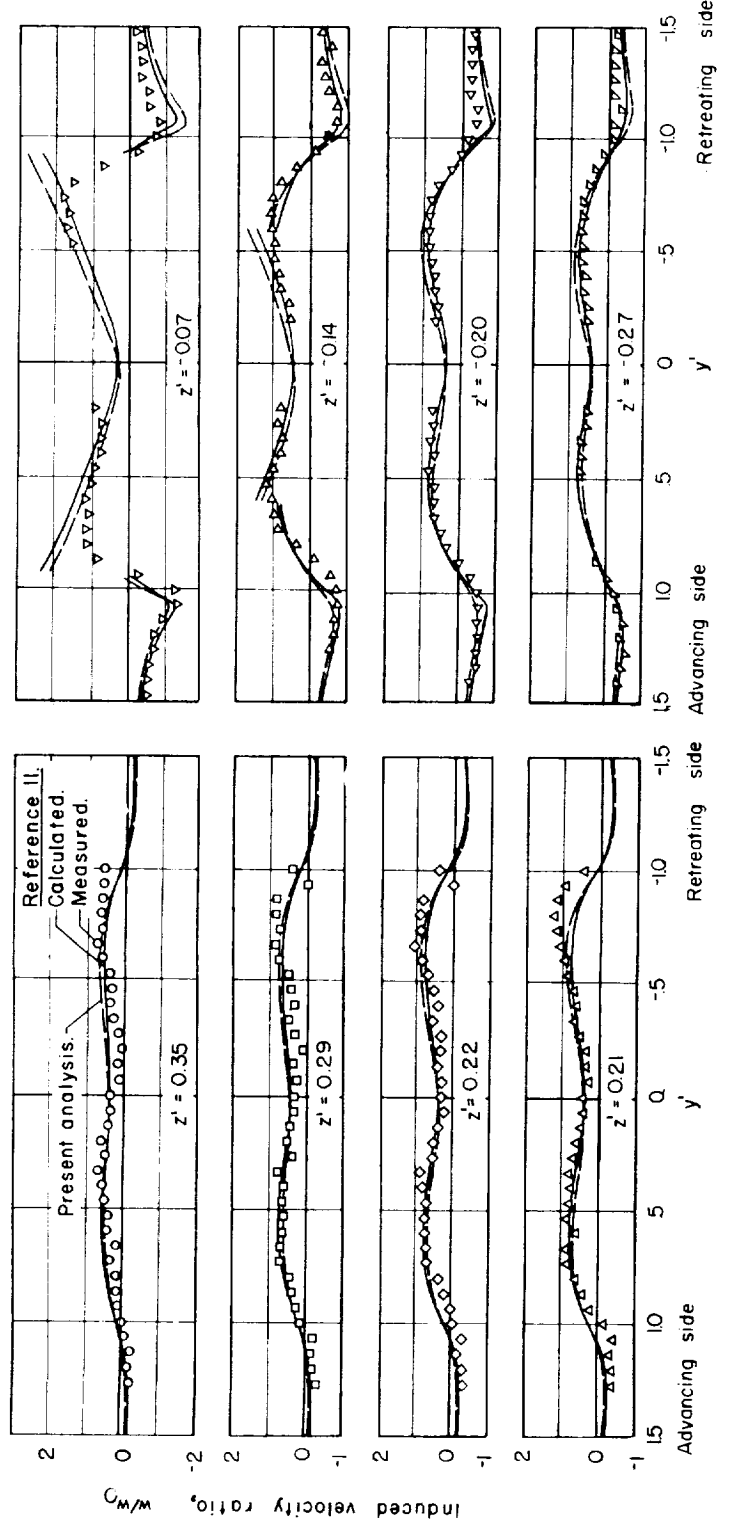
(b) Distribution along axis, $\mu = 0.30$.

Figure 6.- Concluded.



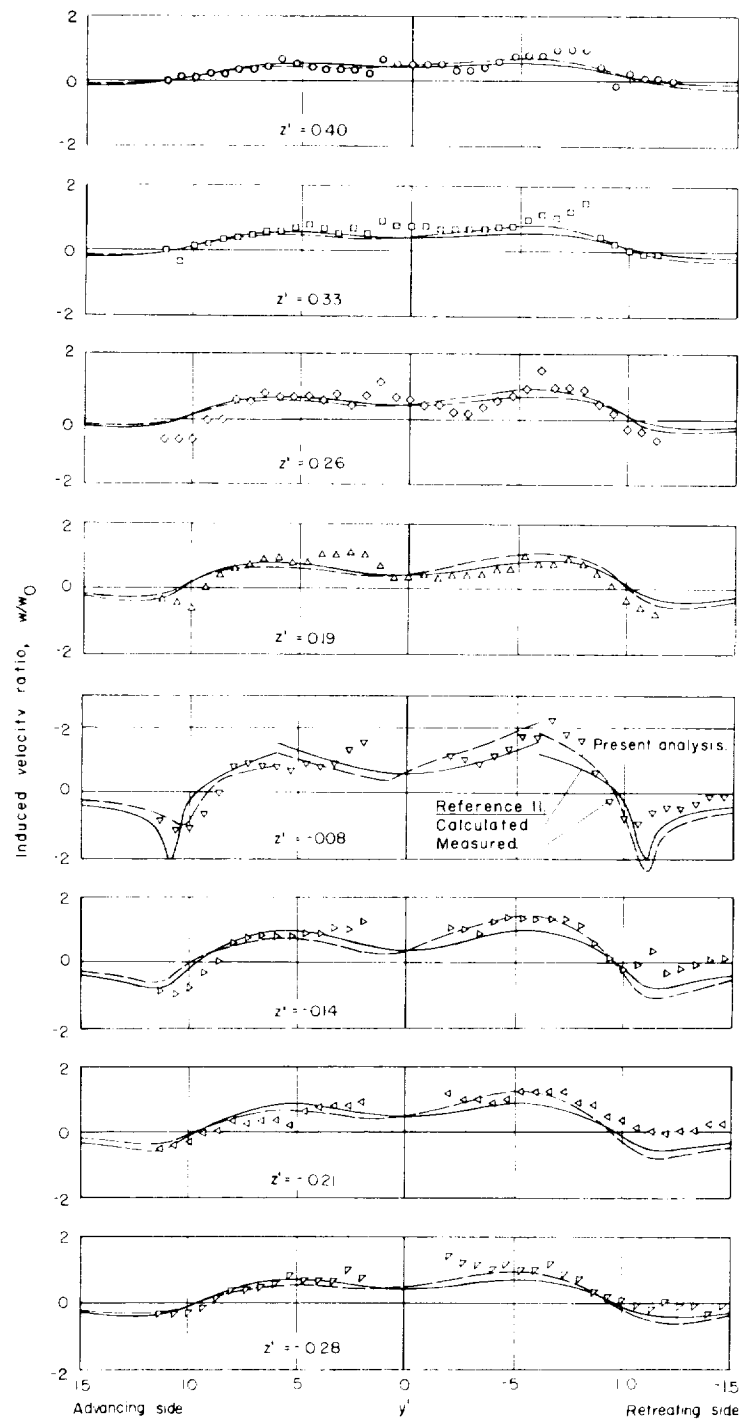
(a) $\mu = 0.095$, $\chi = 75.0^\circ$.

Figure 7.- Comparison, in the lateral plane, of theory and the measurements of reference 11.



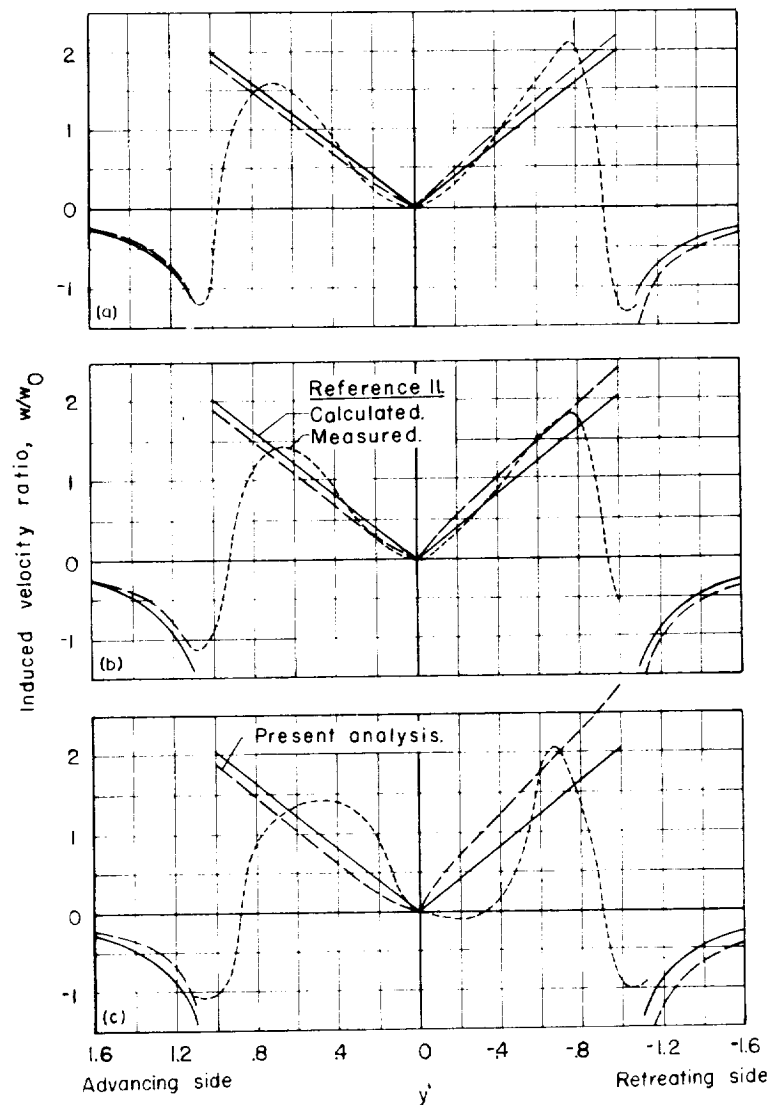
(b) $\mu = 0.140$, $\chi = 82.3^\circ$.

Figure 7.- Continued.



(c) $\mu = 0.232, \chi = 83.9^\circ$.

Figure 7.- Concluded.



(a) $\mu = 0.095, \quad X = 75.0^\circ.$

(b) $\mu = 0.140, \quad X = 82.3^\circ.$

(c) $\mu = 0.232, \quad X = 83.9^\circ.$

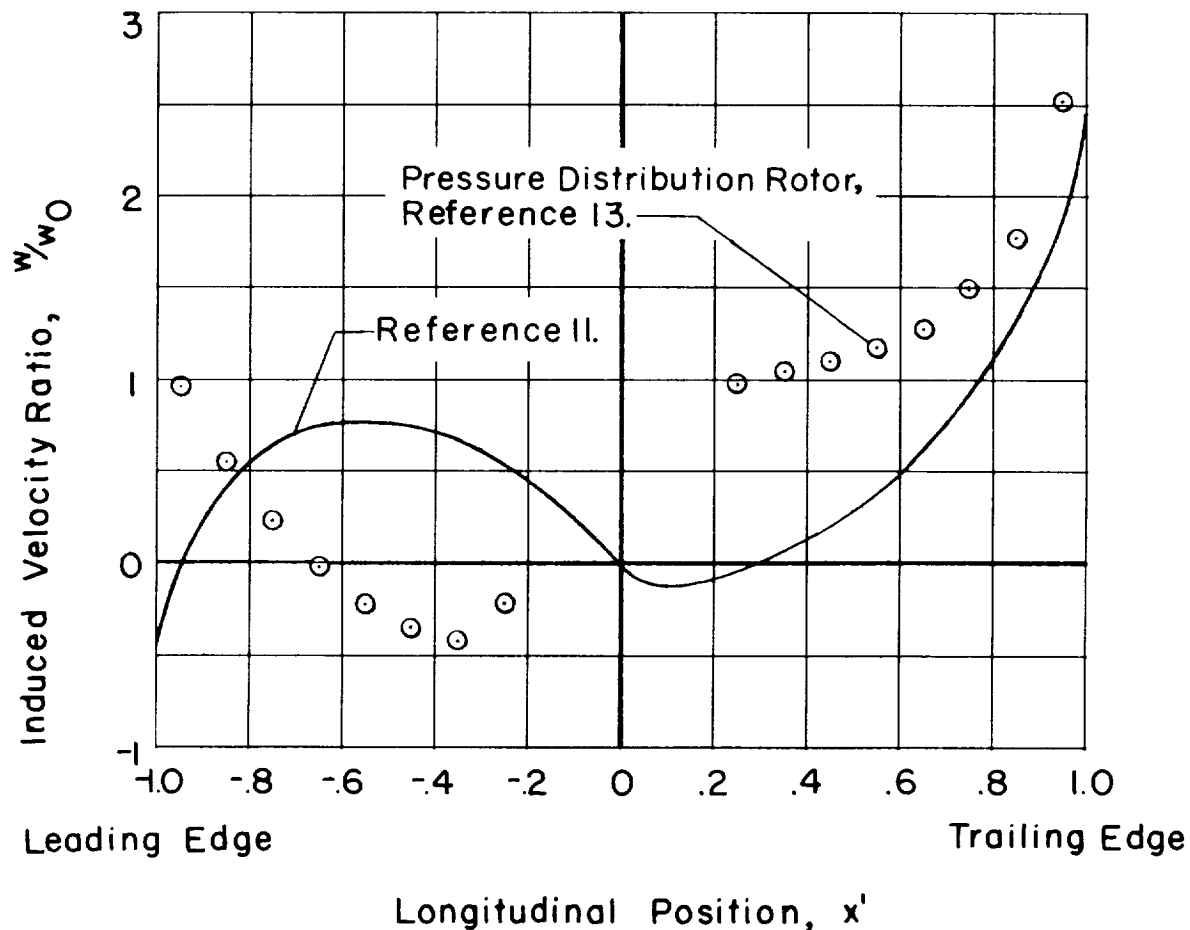
Figure 8.- Comparison, along the lateral axis, of theory and the measurements of reference 11.

EFFECT OF TIP-SPEED RATIO ON INDUCED
VELOCITIES NEAR A LIFTING ROTOR

By Harry H. Heyson

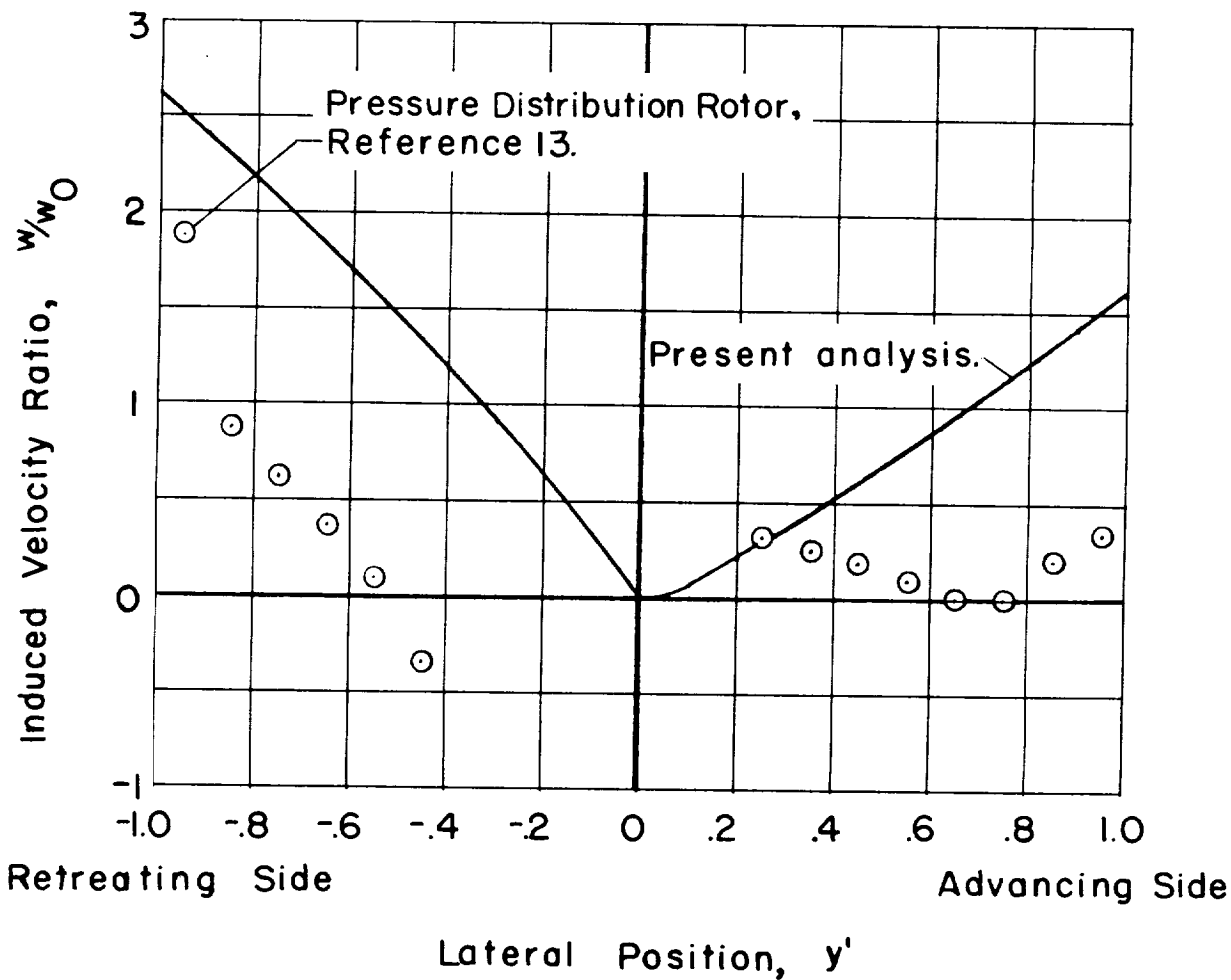
ABSTRACT

A theoretical investigation of the effect of tip-speed ratio and the associated asymmetry of induced flow in the vicinity of a lifting rotor has been conducted. The analysis is based upon an asymmetric wake which is a logical extension of that used for previous investigations. Equations for the induced velocities at an arbitrary point in space are presented in a form suitable for numerical integration. Numerical results for the normal induced velocity in the lateral plane of the rotor are presented in the form of tables and charts. Comparison with previously available measurements indicates an improvement in accuracy over older theories. The results should be useful in estimating the interference between wing and rotor of compound helicopters and convertiplanes. In addition, the results may be applicable to the problem of mutual interference between rotors of multi-rotor helicopters.



(a) Longitudinal axis.

Figure 9.- Comparison of calculated time-averaged induced velocities with effective induced velocities as determined by pressure distribution measurements on a rotor blade (ref. 13). $\mu = 0.30$.



(b) Lateral axis.

Figure 9.- Concluded.

EFFECT OF TIP-SPEED RATIO ON INDUCED
VELOCITIES NEAR A LIFTING ROTOR

By Harry H. Heyson

ABSTRACT

A theoretical investigation of the effect of tip-speed ratio and the associated asymmetry of induced flow in the vicinity of a lifting rotor has been conducted. The analysis is based upon an asymmetric wake which is a logical extension of that used for previous investigations. Equations for the induced velocities at an arbitrary point in space are presented in a form suitable for numerical integration. Numerical results for the normal induced velocity in the lateral plane of the rotor are presented in the form of tables and charts. Comparison with previously available measurements indicates an improvement in accuracy over older theories. The results should be useful in estimating the interference between wing and rotor of compound helicopters and convertiplanes. In addition, the results may be applicable to the problem of mutual interference between rotors of multi-rotor helicopters.